Changing food webs before and during the Last Glacial Maximum based on stable isotopes of animal bone collagen from Lower Austria

Lilian Reiss[1], Christoph Mayr[1, 2], Kerstin Pasda[3], Thomas Einwögerer[4], Marc Händel[4], Andreas Lücke[5], Andreas Maier[6], Holger Wissel[5]

[1] Institute of Geography, Friedrich-Alexander-Universität Erlangen-Nürnberg, Wetterkreuz 15, 91058 Erlangen, Germany

[2] Department Earth and Environmental Sciences & GeoBio-Center, Ludwig-Maximilians-Universität München, Richard-Wagner-Strasse 10, 80333, Munich, Germany

[3] Institute of Prehistory and Protohistory, Friedrich-Alexander-Universität Erlangen-Nürnberg, Kochstrasse 4/18, 91054 Erlangen, Germany

[4] Austrian Archaeological Institute, Austrian Academy of Sciences, Georg-Coch-Platz 2, 1010 Vienna, Austria

[5] Institute of Bio- and Geosciences, IBG-3: Agrosphäre, Forschungszentrum Jülich GmbH, 52425 Jülich, Germany

[6] Institute for Prehistoric Archaeology, University of Cologne, Bernhard-Feilchenfeld-Strasse 11, 50969 Cologne, Germany

Corresponding author: Lilian Reiss (lilian.reiss@fau.de)

Abstract

We investigated palaeo-food web structures using stable isotope analyses on animal bone collagen from four Upper Palaeolithic sites dated to the Early Gravettian (Krems-Hundssteig and Krems-Wachtberg: 33-31k cal a BP, Langenlois: 31-29k cal a BP) and to the Early Epigravettian (Kammern-Grubgraben: 24-20k cal a BP). In both periods, $\delta^{13}C$ values show niche partitioning between hare, horse, and mammoth on the one side, and reindeer and ibex on the other side indicating different diet and habitats between both herbivore groups. The $\delta^{15}N$ differences between carnivores and herbivores suggest a difference of one trophic level during

the pre-Last Glacial Maximum (LGM) period at the Early Gravettian sites and a tendency towards secondary carnivores during the LGM at Kammern-Grubgraben. $\delta^{15}N$ values of pre-LGM mammoths are elevated in relation to other herbivores but shifted to the level of other herbivores in the LGM. A general $\delta^{15}N$ value shift in herbivores of 3.3‰ from the pre-LGM to the LGM is related to climatic deterioration. This may have led to the disappearance of certain ecological niches and to a shift from broader to overlapping ecological herbivore niches shortly before the LGM, as demonstrated by SIBER analyses.

Key Words: $\delta^{13}C$, $\delta^{15}N$, niche partitioning, Gravettian, Epigravettian

1. Introduction

Animal bones represent a frequently well-preserved and widely abundant archive at Palaeolithic sites. Their isotopic composition is commonly used to reconstruct local palaeo-food webs and past ecosystems (Bocherens et al., 2015; Brock et al., 2010; Drucker et al., 2012; DeNiro and Epstein, 1978; Hobson, 1999; Hoke et al., 2019). The reconstruction of food webs is based on the fact that isotopic fractionation occurs between animals from different trophic levels. Moreover, isotopic differences at the baseline of food webs occur across geographical regions and in different climates. Potential shifts in the isotopic composition due to trophic level or geographic origin are well reflected in animal tissues, such as bone collagen (DeNiro and Epstein, 1978; Hobson, 1999).

For bone collagen, carbon stable isotopes show a trophic enrichment of approximately 0.8-1.3‰ in carnivores in comparison to their prey (Bocherens and Drucker, 2003; Krajcarz et al., 2016), whereas nitrogen stable isotopes increase more significantly with about 3.0-5.0‰ enrichment per trophic level (DeNiro and Epstein, 1981; Schoeninger and DeNiro, 1984; Bocherens and Drucker, 2003; Fox-Dobbs et al., 2007). Unlike tooth dentin with its incremental growth, bone is a renewing tissue, so that its isotopic composition exhibits an averaged value over several years of nutritional behaviour (Drucker 2022). The collagen in femoral bones of human adults, for instance, reflects a period of more than a decade (Hedges et al., 2007).

A number of stable isotope studies on bone collagen have been conducted for the steppe- and tundra-like ecosystems of the last glacial period in Central Europe, in particular for Marine Isotope Stage (MIS) 3 (59-29k cal a BP) and MIS 2 (29-11.7k cal a BP) (Voelker et al., 2002). Due to the predominance of large herbivorous mammals, this ecosystem is also known as

60 “mammoth steppe” (e.g., Zimov et al., 1995, 2012; Bocherens, 2003; Bocherens et al., 2005,
61 2014, 2015; Drucker et al., 2003; Drucker and Henry-Gambier, 2005; Fox-Dobbs et al., 2008;
62 Yeakel et al., 2013, Schwartz-Narbonne et al., 2019). This biome is characterised by a large
63 biomass of plants and herbivores despite the partly very cold and dry conditions during the last
64 glacial. It has been proposed that high insolation and low humidity led to increased summer
65 snowmelt and a longer growing season (Guthrie, 1982; Zimov et al., 2012; Drucker, 2022). A
66 rapid turnover of nutrients in loess sediments may also have favoured high vegetation
67 productivity and, thus, provided the base for grazing and browsing by animal communities,
68 which in turn fertilised the soils through manure and carcasses (Zimov et al., 1995; Drucker,
69 2022). Depending on the geographic region and the time period considered, the Eurasian
70 mammoth steppe is characterised by a changing landscape of continuous and discontinuous
71 permafrost (Delisle et al., 2007; Blaser et al., 2010; Vandenberghe et al., 2014). According to
72 Řičánková et al. (2015), the Altai-Sayan, Kazakhstan, and the Eastern European Plain are the
73 areas that best serve as modern equivalents.

74 The isotopic composition of a number of faunal assemblages from the late MIS 3 and MIS 2
75 suggests a particular niche partitioning. This may have been caused by the great diversity of
76 coexisting herbivores and interspecies competition (Iacumin et al., 2000, 2006; Drucker et al.,
77 2003; Bocherens et al., 2015; Drucker, 2022). Based on $\delta^{15}N$ and $\delta^{13}C$ value ranges, ecological
78 niches of mammoth, horse, and reindeer were most frequently investigated in different regions.
79 Most studies on faunal composition and food web structures use material from Gravettian (33-
80 25 ka) and Magdalenian (20-14 ka) sites (Iacumin et al., 2000, 2006, 2010; Drucker et al., 2003,
81 2018; Stevens and Hedges, 2004; Stevens et al., 2008; Bocherens et al., 2015; Krajcarz et al.,
82 2016; Fox-Dobbs et al., 2008) and thus focus on the periods before and after the Last Glacial
83 Maximum (LGM). Here we use Mix et al.'s (2001) definition of the LGM *sensu stricto*, which
84 sets it at 23-19k cal a BP. Studies about the food-web structure for the LGM are largely absent.
85 From an archaeological perspective, the transition from the Gravettian to the Epigravettian is
86 of great interest, as human population in Central Europe decreased massively and human
87 occupation remained at very low numbers and densities in the research area during the LGM
88 (Maier et al., 2021).

89 The aim of this study is to infer possible food web changes related to climatic and environmental
90 trends around the LGM using carbon and nitrogen stable isotopes of animal bone collagen. For
91 this purpose, we use the diverse faunal assemblages from different well-known Upper

Palaeolithic sites in and nearby the city of Krems (Lower Austria) which date to 33–29k cal a BP (Early Gravettian/pre-LGM) and 24–20k cal a BP (Early Epigravettian/LGM). The geographic proximity of the sites allows meaningful conclusions from a comparison between the different age periods.

2. Study sites

2.1 Krems-Hundssteig 2000-2002 and Krems-Wachtberg 1930 (33–31k cal a BP)

The Upper Palaeolithic sites of Krems-Hundssteig and Krems-Wachtberg are located very close to one another, both in the present-day urban area of the city of Krems (Fig. 1). Topographically, the sites are situated at the transition from the narrow Danube passage of the Wachau to the so-called Tullnerfeld, an extensive alluvial plain. They are located in the lower southern to south-eastern part (Wachtberg) of a spur-shaped promontory that elevates up to 398 m a. s. l. on the northern bank of the Danube. The Wachtberg area, where loess deposits are up to 20 metres thick, is slightly sloping to the southeast, thus providing wind protected conditions for temporarily used campsites of hunter-gatherer communities (Händel, 2017).

The Upper Palaeolithic site of Krems-Hundssteig first received attention in the late 19th century. At that time, numerous lithic artefacts and faunal remains were found in the course of large-scale quarrying of loess sediments. The lithic industry points at Aurignacian and Gravettian. New excavations have been carried out adjacent to the former quarry area between 2000–2002 and identified five basic archaeological horizons (AH). The main Upper Palaeolithic horizon, AH 3, is attributed to the Gravettian and represents a sequence of layers that can be subdivided in an upper (AH 3.1 and AH 3.2), middle (AH 3.3–AH 3.4) and lower sequence (AH 3.5–AH 3.8) (Neugebauer-Maresch et al., 2008). All bone samples analysed herein originate from the Krems-Hundssteig 2000-2002 excavations and stem from AH 3.2 and 3.4, which date between 32.9–31.0k cal a BP (Fig. 2a). Radiocarbon dating from two lower horizons, accessed only by sounding and core sampling, exhibited age ranges of 38.9–34.5k cal a BP for AH 4 and 46.6–42.4k cal a BP for AH 5 (Neugebauer-Maresch et al., 2008; Händel 2017). From a zooarchaeological point of view, Krems-Hundssteig 2000-2002 is mainly characterised by a low abundancy of carnivores in contrast to the neighbouring Krems-Wachtberg sites (Fladerer and Salcher-Jedrasiak, 2008). The faunal assemblage of Krems-Hundssteig considered here (AH 3.21, 3.22, 3.24, and 3.44) predominantly consists of mammoth, reindeer, and horse with

minor contributions of red deer, woolly rhinoceros, arctic fox, wolf, and hare, as well as micromammals. The minimum number of individuals (MNI) for the relevant horizons was 57 (Fladerer and Salcher-Jedrasiak, 2008; Händel, 2017).

During excavations in the 1930s, numerous lithic artefacts and animal remains, including mammoth tusks, were found at the Gravettian site of Krems-Wachtberg 1930 (Einwögerer, 2000; Fladerer, 2001). Although three find layers have been observed during the excavation, the recovered material was not separated. Thus, all samples must be considered as one complex and radiocarbon ages (33.4–31.0k cal a BP) point to an Early Gravettian occupation more or less contemporaneous to Krems-Wachtberg 2005-2015 (Fig. 2b; Einwögerer et al., 2009; Händel, 2017). The faunal remains comprise mainly mammoth, wolf, red and arctic fox and wolverine and to a lesser extent red deer, reindeer, ibex and musk ox (MNI = 28; Fladerer, 2001; Händel, 2017).

The loess records of Krems-Wachtberg 2005-2015 were studied sedimentologically and indicate a climatic deterioration around the MIS 3-MIS 2 transition (Sprafke et al., 2020) as indicated also elsewhere in Central Europe (Stojakowits et al., 2021).

2.2 Langenlois A (31–29k cal a BP)

The Upper Palaeolithic site Langenlois is located in the area of a former brickyard in the southeast of the town of Langenlois (Fig. 1). The find locations Langenlois A–C are located on a loess-covered slope exposed to the east and facing towards the river Kamp. Placed in a valley basin, the site is protected to the north by smaller hills and to the southwest by the prominent Gobelsberg elevation. During the first excavations of the site Langenlois A in the early 1960s, one archaeological horizon was identified, which is characterised by different occupational structures. Three adjacent fireplaces, an unevenly developed cultural layer, and various other features, such as workplaces for the fragmentation of bones, suggest a variety of activities. All specimens analysed here originate from the excavation site Langenlois A and date to 30.8–29.2k cal a BP (Fig. 2c; Einwögerer, 2019). The faunal assemblage is dominated by ibex, followed by horse and reindeer plus a few remains of red deer and mammoth (Einwögerer, 2000).

2.3 Kammern-Grubgraben (24–20k cal a BP)

At the Kammern-Grubgraben site, Upper Palaeolithic finds were first collected in 1890 (Spöttl, 1890; Obermaier, 1908; Händel et al., 2021a). However, it was not until 1985 that systematic

excavations (1985–1990) began in the area of the present excavation site (Brandtner, 1990, 1996; Montet-White, 1988, 1990). During an inventory project in 2013, 23,000 inventory numbers were assigned, which comprise archaeological and zooarchaeological material (Neugebauer-Maresch et al., 2016). A new phase of field investigations began in 2015, which is still ongoing (Händel et al., 2021a).

Kammern-Grubgraben is one of few stratified LGM sites in Central Europe and is located in the south-eastern extension of the Moravian-Bohemian Hills (Fig. 1; Händel et al., 2021a). It is situated on a gentle loess-covered slope between two hills, the Heiligenstein in the east and the Geißberg in the west. The site is open towards the south, i.e., to the Kamp River valley and the Danube plain and confined towards the northwest by the adjacent Moravian plateau. Given the harsh environmental conditions during the LGM (Maier et al., 2021; Händel et al., 2021a), this geographic setting may have been advantageous for hunter-gatherer communities, given the wind protection and proximity to water. Sedimentological studies at Kammern-Grubgraben indicate a rather monotonous depositional environment during the LGM, dominated by aeolian deposition of silt-sized loess (Reiss et al., 2022).

Beside lithic and organic artefacts, the Kammern-Grubgraben inventory also includes a large number of faunal remains. The faunal assemblage of Kammern-Grubgraben is dominated by reindeer, followed by horse at a large distance. Minor contributions of hare, mammoth, bison, red deer, ibex, wolf, brown bear, wolverine, arctic fox, red fox, goose, and gopher occur (MNI=234; Pfeiffer et al., accepted). The zooarchaeological material stems from different archaeological layers, which were addressed differently in various excavation campaigns during the long period of research. The samples analysed here originate from both the Brandtner excavation and the excavation led by the team of Montet-White. Therefore, the labelling of the find horizons varies depending on the excavation year. The Montet-White and Brandtner excavations documented five consecutive archaeological layers (AL 1-5) and assigned these to at least five different occupation phases (Haesaerts et al., 2016; Neugebauer-Maresch et al., 2016). However, more recent investigations indicate that former AL's 2-4 likely represent a single main occupation phase, here referred to as AH 2. The earlier AH 3 (probably corresponding to former AL 5) seems to represent a much less intensive occupation, while AH 1 (former AL 1) at least partly contains relocated finds and suggests contributions from different occupational episodes including a younger, potentially Magdalenian, occupation. Radiocarbon

ages of faunal remains (bones and teeth) from AH 1 and 2 (resp. AL 1-4) indicate human activity between 23.7-19.5k cal a BP (Fig. 2d,e; Haesaerts et al., 2016; Händel et al., 2021a).

3. Material and methods

3.1 Bone material

The find inventories include large numbers of faunal remains, both bones and teeth, of terrestrial animals, including various carnivores (red fox, arctic fox, wolf, and wolverine) and numerous herbivores (woolly mammoth, reindeer, red deer, horse, bison, musk ox, woolly rhinoceros, hare, ibex, and goose). Bone material was sorted according to stratigraphic aspects and taxonomically identified by K. Pasda for Kammern-Grubgraben and Langenlois. The faunal remains from Krems-Hundssteig 2000-2002 had already been taxonomically identified and documented by Fladerer and Salcher-Jedrasiak (2008) and the Krems-Wachtberg 1930 inventory by Fladerer (2001). To avoid samples with potentially poor collagen preservation, bones with a compact texture were selected preferentially for collagen extractions and subsequent stable isotope analyses.

In most cases, the same species were selected from the inventories to allow for accurate comparisons between species and sites. Whenever possible, different individuals of a species were selected from one site (Table 1). In order to increase the number of species and to obtain as many species as possible for both periods, the food webs of the Early Gravettian sites Krems-Wachtberg 1930 (KW) and Krems-Hundssteig 2000-2002 (HU) are combined and discussed as one coherent food web (KW+HU) in comparison to the Early Epigravettian food web of Kammern-Grubgraben (KG). This decision is justified for KW and HU based on spatial proximity (less than 250 m) and identical ^{14}C age range (Fig. 2a,b). In addition, we included the site Langenlois A (LK), nine km northeast of KW+HU, in this study because it contains a considerable number of ibexes, which are rare in KW+HU but also common in KG. LK appears around 2k years younger than KW+HU, although its age range overlaps with these sites (Fig. 2c).

In the evaluation and discussion, only bone-collagen data is considered, as the values of dental collagen can be considerably enriched in ^{15}N compared to bone collagen, which has been confirmed for dental collagen from reindeer (Fizet et al., 1995; Britton, 2010). In addition to bone collagen analyses from KG-AH 2, four samples from KG-AH 1 were analysed, but these

results are not included in the discussion, as it cannot be excluded that they originate from a Magdalenian, i.e., post-LGM occupation. Both dental collagen values and samples originating from KG-AH 1 were not further considered but are listed in Supplementary Table S1 for completeness.

3.2 Fourier-transform infrared (FTIR) spectroscopy

FTIR spectroscopy was used as a pre-screening method on a defined set of samples (KG: n=7, HU: n=4, KW: n=4, LK: n=3) of bone powder to detect the preservation of collagen (Cersoy et al., 2016; Lebon et al., 2016). It was further applied on the respective extracts to check for chemical purity of bone collagen. Less than 2 mg of each powdered sample were used for FTIR spectroscopy in attenuated total reflectance (ATR) mode (IR Prestige-21, Shimadzu). The device parameters were set according to the method of Lebon et al. (2016). Infrared spectra were obtained from 64 scans per run with a spectral resolution of 2 cm^{-1} in the wavenumber range of 4000–370 cm^{-1}. To account for sample heterogeneity and to determine instrumental reproducibility, each sample was measured in triplicates. Prior to every sample measurement, a new baseline (air, CO_2) was set. Wavenumbers in the range of 1710 to 1590 cm^{-1} and 1110 to 940 cm^{-1} represent the amide I band and the $_{v3}$phosphate ($_{v3}PO_4$)-band, respectively (Lambert et al., 1998; Lebon et al., 2016).

3.3 Collagen extraction

Collagen extraction followed a slightly modified version of the method of Bocherens et al. (1991). About 0.5-2.0 g were carefully sawn from each animal bone using a rotary tool (Proxxon-Micromot, Germany) with a circular diamond blade. Wherever necessary, samples were cleaned with sandpaper and a common toothbrush before soaking them in deionized water for 30 minutes. Samples that were hardened or glued for preservation were additionally soaked in acetone to remove varnishes from the bones.

Subsequently, samples were ultrasonically cleaned in deionized water for 10 seconds and dried in a drying oven at 40 °C overnight. Samples were then ground using a mortar and a pestle. 0.25 to 1.0 g of each powdered sample (0.3-0.7 mm grain size) was weighed in centrifuge tubes and soaked in 1 M HCl. To dissolve minerals, samples were shaken on a rotator for 20 minutes. Subsequently, samples were repeatedly washed with distilled water and centrifuged (Heraeus Multifuge 3L-R, Thermo Electron Corporation, USA) at 3000 rpm for five minutes, respectively, until a pH of 6 was reached. For dissolution of humic acids, the pellets were soused

with 0.125 M NaOH and left under the fume hood for 20 hours. Thereafter, all samples were washed again with distilled water and centrifuged until pH was neutral. In the last step, the pellets were soaked in 0.01 M HCl (pH 2) and incubated for 10-17 hours in a water bath (Julabo, SW23, Germany) at 95 °C to solubilize the gelatine.

Finally, the dissolved gelatine was filtrated through MF-Millipore membrane filters (5.0 µm), using vacuum flasks and filter funnels, frozen and lyophilised.

3.4 Stable isotope analysis

Samples were analysed in duplicates or triplicates at the stable isotope laboratories at Forschungszentrum Jülich (FZJ) and Friedrich-Alexander-Universität Erlangen-Nürnberg (FAU), respectively. 240–260 µg of collagen was wrapped in tin capsules and combusted in an elemental analyser (Flash2000, Thermo Fisher, USA, FZJ; NC 2500, Carlo Erba, Italy, FAU) and measured online with a coupled isotope ratio mass spectrometer (DeltaV plus, Thermo Fisher, USA, FZJ; DeltaPlus, Thermo-Finnigan, Germany, FAU). Carbon and nitrogen measurements were performed within one analysis run on the same sample.

Isotope results are reported as delta (δ) values in per mil (‰) according to the equation:

$$\delta = R_S / R_{St} - 1.$$

R_S is the isotope ratio ($^{13}C/^{12}C$, $^{15}N/^{14}N$) of the sample and R_{St} of the respective standard. δ-values are normalized to VPDB (Vienna Pee Dee Belemnite) scale for carbon and AIR (atmospheric nitrogen) scale for nitrogen (Coplen 2011).

Calibration of laboratory standards and scale-normalisation of $\delta^{13}C$ raw values is based upon the International Atomic Energy Agency (IAEA) reference standards IAEA-CH6 ($\delta^{13}C$=-10.45‰) and IAEA-CH7 ($\delta^{13}C$=-32.15‰), and the United States Geological Survey (USGS) standard USGS24 ($\delta^{13}C$=-16.05‰). The average standard deviation of replicate measurements for $\delta^{13}C$ standards measured in the respective runs was 0.24‰ for IAEA-CH7 (n=8), 0.48‰ for USGS41 (n=8) and 0.10‰ for the laboratory standard peptone (n=8).

Calibration of laboratory standards and scale-normalisation of $\delta^{15}N$ raw values is based upon the international reference standards IAEA-N-2 ($\delta^{15}N$=20.3‰), IAEA-N-1 ($\delta^{15}N$=0.4‰) and USGS25 ($\delta^{15}N$=-30.4‰). The average standard deviation of replicate measurements of $\delta^{15}N$ standards measured in the respective runs was 0.28‰ for IAEA-N-1 (n=8), 0.15‰ for IAEA-N-2 (n=8), 0.14‰ for lab standard peptone (n=8), and 0.15 ‰ for USGS41 (n=8). Samples

were also analysed for their weight percentage carbon (%) and nitrogen (%) using elemental standards for calibration. The measurement error of the element concentrations was <5%. Elemental contents and atomic C/N ratios were used to check for chemical purity.

3.5 Quality criteria for collagen preservation

Impurities or diagenesis may lead to a shift in the isotope values of prehistoric bone collagen. The C/N ratio is known to be a quality criterion for collagen and was used to validate collagen purity (Guiry and Szpak, 2021). Reported C/N ratios for pure collagen vary between 2.9 and 4.0 (DeNiro, 1985; Grupe et al., 2003; Coltrain et al., 2004; Bösl et al., 2006; Hoke et al., 2019), but samples with C/N >3.6 should be rejected as the collagen purity for those cannot be guaranteed (van Klinken, 1999; Ambrose, 1990).

Another quality criterion used was collagen yield and element contents. According to DeNiro and Weiner (1988) the minimum yield of extracted collagen (wt.%) should be 2%, but more recent studies suggest 1% (Ambrose, 1990, Ambrose and Norr, 1993; Dobberstein et al., 2009) or even 0.5% (van Klinken, 1999) as sufficient for acceptable preservation (Hoke et al., 2019). The nitrogen and carbon contents of unaltered collagen are 11-16 wt% and 35±9 wt%, respectively, (van Klinken, 1999) and were used as additional criteria for the quality of the extracted collagen.

3.6 Statistics

Statistical calculations were carried out with R studio (version R-4.2.2). Shapiro-Wilk tests were used to check for normal distribution of data. Possible outliers were determined using Grubb's tests. Wilcoxon-Mann-Whitney tests were carried out to test the null hypothesis of whether two groups are statistically indifferent (Dytham, 2011). For all analyses performed, a significance level of 0.05 was chosen.

Comparisons of isotopic niches among different animal communities were analysed using the Stable Isotope Bayesian Ellipses in R (SIBER) package (Jackson et al., 2011). It must be emphasised here that isotopic niches do not necessarily correspond to ecological niches, since, for example, different trophic niches can lead to the same isotopic ranges (Jackson et al., 2011). In comparison to simple convex-hull methods, SIBER is based on multivariate ellipse metrics, with the advantage of being independent of sample size while enabling robust comparison between data sets of different sizes (Jackson et al., 2011).

We calculated convex hulls, i.e., total area (TA) and standard ellipse area (SEA, in ‰²) of herbivorous taxa represented by more than three data points. For the KW+HU and KG food webs, these include horse, hare, reindeer, and woolly mammoth, for LK and KG ibex. The SEA explains 40 % of all potential specimens that fit into the respective niches, based on a Bayesian probability estimation. The SEA is sensitive to sample size, which is why we used the recommended standard ellipse area corrected for sample size (SEAc) (Jackson et al., 2011).

4. Results

4.1 Preservation and purity of collagen

FTIR spectra revealed a sufficient amount of collagen in all powdered bone samples analysed (Fig. 3a). The FTIR spectra of the powdered untreated samples show a distinct peak in the amide I band range (1710 to 1590 cm^{-1}) indicative for collagen, while the $_{v3}PO_4$ band range (1110 to 940 cm^{-1}), indicative for bone phosphate (PO_4), is obviously more pronounced.

Collagen quality was confirmed by FTIR spectra of the extracted collagen of selected samples (Fig. 3b). After collagen extraction, no $_{v3}PO_4$ band could be detected anymore, indicating complete dissolution of $_{v3}PO_4$ during collagen extraction procedure. Instead, the amide band is most pronounced, indicating pure collagen was extracted.

Collagen yields (wt.%), varied between 0.8 to 16% and were on average 4.3% at KG and 7.0% at KW. Two samples (woolly mammoth ‘KG 1110’ and ibex ‘KG 249’) yielded collagen contents <0.5%. However, other chemical characteristics, such as %N, %C and C/N ratios of these samples, are still within the acceptable range for well-preserved collagen, except for KW-MK-938 (red fox), KG-2652 (bison), and KG-1500 (hare), which had too low nitrogen and carbon contents (Table S1). All other samples are thus considered reliable in terms of collagen preservation and included in the further evaluation. The high purity of all extracted collagen samples was generally confirmed by their C/N ratios which range between 2.9 and 3.6 as expected for pure collagen (Table S1).

4.2 Isotopic results of bone collagen

All stable isotope results are shown in $\delta^{15}N$-vs.-$\delta^{13}C$ plots separated for the Early Gravettian/pre-LGM sites KW+HU (Fig. 4a), the Early Gravettian/pre-LGM site LK (Fig. 4b) and the Early Epigravettian/LGM site KG (Fig. 4c). Shapiro Wilk tests confirm a normal

distribution of the complete dataset ($\delta^{15}N$: W=0.97455, p<0.05 and $\delta^{13}C$: W=0.9042, p<0.05). We excluded one outlier (hare 'WA-MK 923', confirmed by Grubb's test) from further evaluations and listed it only in Supplementary Table S1, as the exceptionally low $\delta^{13}C$ values most likely point to modern contamination.

In the pre-LGM food web of KW+HU, all common herbivorous species except mammoth exhibit mean $\delta^{15}N$ values between 2.1±1.2 (hare) and 5.3±2.3‰ (woolly rhinoceros). Musk ox also exhibits a very high $\delta^{15}N$ value of 7.7‰, respectively. However, they are represented by only one specimen and therefore may not be representative. As mentioned, mammoths exhibit considerably higher $\delta^{15}N$ values than other herbivores, with a mean value of 8.2±0.8‰ and are thus almost on the same level as the carnivorous species wolf and wolverine that exhibit $\delta^{15}N$ mean values of 8.8±0.7 and 8.8±1.1‰, respectively (Fig. 4a). Arctic fox and red fox show slightly lower $\delta^{15}N$ mean values of 7.5±1.2 and 7.2±0.4‰.

In the pre-LGM food web of LK, hare exhibits a mean $\delta^{15}N$ value of 3.6±0.1‰, reindeer of 4.7±3.9‰, horse of 3.5±0.9‰, and ibex of 4.7±0.7‰. Single specimens of red deer and goose exhibited $\delta^{15}N$ values of 2.8 and 7.0‰.

At the LGM site KG, $\delta^{15}N$ mean values of herbivore taxa range from 1.8±0.7 in hare to 3.9‰ in goose, which is again represented by only one specimen (Fig. 4b). The highest single values of herbivores belong to infantile individuals of ibex and horse (3.6 and 3.5‰, respectively). In contrast to the pre-LGM sites, the $\delta^{15}N$ values of mammoth (2.5±0.9‰) at KG are in the range of other herbivores. Carnivores show $\delta^{15}N$ mean values of 7.5±2.4‰ and are thus 5.2‰ higher than herbivores. However, arctic fox's $\delta^{15}N$ values are highest but exhibit a large scatter (8.6±3.2‰), while wolf (7.3±1.9‰), red fox (6.7‰) and wolverine (5.9‰) show lower values.

A comparison between pre-LGM (KW+HU, LK) and LGM (KG) isotope-derived food webs shows similarities but also some differences. The main similarity between both periods is a separation between two clusters of herbivores: in KW+HU and KG horse and hare have generally lower $\delta^{13}C$ values than the cluster formed by ibex and reindeer (Fig. 4a,c). In LK the data on hares, reindeer and horses are too small to draw such a conclusion. Red deer exhibits a varying position in $\delta^{15}N$-versus-$\delta^{13}C$ space: in the pre-LGM period at KW+HU it falls between the fields of rhinoceros and horse on the one side, and hare on the other side(Fig. 4a), while in the LGM it plots together with reindeer and ibex (Fig. 4c). The most striking difference between pre-LGM (KW+HU) and LGM (KG) is, however, the shift of the mammoth cluster mainly related to the strong $\delta^{15}N$ decrease between both periods as already mentioned above. During

the pre-LGM period, the cluster of mammoths does not match any of the herbivores except a single musk ox bone, while the data cluster overlaps with those of horses and hares in the LGM.

For better evaluation, we statistically tested the isotopic differences between pre-LGM and LGM sites for the most common herbivorous taxa, i.e., mammoth, horse, hare, reindeer, and ibex using the Wilcoxon-Mann-Whitney test (Fig. 5a,b). All tested pairs belonged to KW+HU versus KG, except for ibex, for which LK versus KG was used. With the exception of hare, all taxa had significantly higher $\delta^{15}N$ values in the pre-LGM than in the LGM (Fig. 5a).

In terms of absolute values, a marked $\delta^{15}N$ shift occurs between both periods except for hare. In the pre-LGM period, $\delta^{15}N$ mean values of all herbivores are on average 3.3‰ higher than in the LGM food web. If mammoth is excluded, the shift is still 2.0‰.

Detailed statistical analyses demonstrate that only $\delta^{13}C$ of mammoth is significantly different between both periods and exhibits the lowest $\delta^{13}C$ values in the pre-LGM period of KW+HU (Fig. 5b). In KW+HU, $\delta^{13}C$ mean values of herbivores range from -21.2±0.2‰ in mammoth to -19.4±0.7‰ in reindeer, showing a slightly broader range compared to the LGM (-20.8 in goose to -19.6±0.4‰ in reindeer). The largest $\delta^{13}C$ shift between both periods occurs in mammoths from -21.2±0.2 in the pre-LGM period to -20.3±0.4‰ in the LGM. Wolf and wolverine in KW+HU exhibit $\delta^{13}C$ mean values of -19.7±0.4 and -19.7±0.1‰, while arctic fox and red fox show slightly lower $\delta^{13}C$ mean values of -20.2±0.4 and -20.5±0.2‰, respectively. In the LGM, carnivores exhibit $\delta^{13}C$ mean values ranging from -20.0±0.1‰ in arctic fox to -18.7‰ in wolverine (Fig. 4a).

In comparison to the LGM, results of SIBER analyses for the pre-LGM confirm larger isotopic niche widths for all analysed herbivores but mammoth. Mammoth has a SEAc of 0.6‰² in the pre-LGM (KW+HU) compared to 0.9‰² in the LGM. The SEAc of the other pre-LGM herbivores range from 0.9 (ibex, LK) to 3.1‰² (horse, KW+HU), while in the LGM the same species have SEAc of 0.5 and 0.7‰², respectively (Fig. 6). When considering the isotopic niche areas of both periods, the isotopic niche of ibex is the least variable. Horse shows the largest isotopic niche in the pre-LGM and the biggest change in isotopic niche width between pre-LGM and LGM (Fig. 6).

5. Discussion

5.1 Herbivore niche partitioning indicated by $\delta^{13}C$

Niche partitioning can generally reflect a spatial separation in terms of different habitats, distinct dietary habits, temporal variation, or even temporal and spatial avoidance (Kronfeld-Schor et al., 2001; Stewart et al., 2003; Britton et al., 2012; Bocherens et al., 2015). Herbivore data in the pre-LGM period show a larger variability and thus partly broader isotopic niches in the SIBER analysis than during the LGM (Fig. 6a). This is best explained by the climatic deterioration that significantly affected the environment and consequently the stable isotope pattern of herbivores (Zimov et al., 2012; Drucker et al., 2018; Drucker, 2022).

In comparison to the $\delta^{15}N$ values, the $\delta^{13}C$ clustering of herbivores (with the exception of mammoths) is relatively stable over time (Fig. 5b) and can be directly linked to their dietary habits that are determined by the regional plant communities – except for migratory mammals. The $\delta^{13}C$ results point to two main groups of herbivores: horse and hare show lower, and reindeer and ibex higher $\delta^{13}C$ values (Fig. 5b). Mammoth belongs to the first group during the LGM but has lower $\delta^{13}C$ values than all other taxa in the pre-LGM (Fig. 5b). In (modern) arctic environments, various plant groups show different isotopic compositions (Nadelhoffer et al., 1996; Stevens et al., 2004). Isotope values of modern plant communities from different arctic locations that include grasses, sedges, forbs, shrubs, mosses, fungi, and lichen differed significantly in both, $\delta^{15}N$ and $\delta^{13}C$ values (Barnett, 1994; Wang and Wooller, 2006; Munizzi, 2017; Drucker, 2022). Forbs, graminoids, and fungi show the highest $\delta^{15}N$ values. Shrubs, forbs, and graminoids (grasses and sedges) exhibit the lowest $\delta^{13}C$ values, while lichen shows the highest $\delta^{13}C$ values (Fizet et al., 1995; Finstad and Kielland, 2011). In times when other food sources are deficient, reindeers are thought to consume high proportions of lichen which explains their high $\delta^{13}C$ values (Fizet et al., 2015; Drucker et al., 2001; Bocherens, 2003; Stevens et al., 2008; Finstad and Kielland, 2011; Bocherens et al., 2015). Consequently, previous observations of high $\delta^{13}C$ values in fossil reindeer bones at various locations, such as Belgium (Bocherens et al., 2001; Germonpré et al., 2009), Germany (Stevens et al., 2009; Drucker et al., 2011), France (Fizet et al., 1995; Drucker et al., 2000, 2003; Bocherens, 2003; Drucker and Henry-Gambier, 2005; Bocherens et al., 2005, 2011; Drucker, 2022) or Beringia, i.e., Siberia (Iacumin et al., 2000) and Alaska-Yukon (Fox-Dobbs et al., 2008), were explained by a high proportion of lichen consumption. As ibex falls into the cluster of reindeer, a diet similar to that of reindeer could also be considered for ibex during the glacial, although nowadays the diet of European *Capra ibex* consists mainly of graminoids (Parrini et al., 2009). However, it is known that the Siberian ibex (*Capra sibirica*) in the Altai Mountains preferentially feeds on lichens (Fedosenko and Blank, 2001).

The observed dietary $\delta^{13}C$ differences are likely related to different habitats. As carbon isotope fractionation is driven by distinct pathways of photosynthesis, C_3 and C_4 plants can be easily distinguished by their $\delta^{13}C$ values (Farquhar et al., 1989). However, the presence of substantial amounts of C_4 plants in the investigated region during the last glacial can be excluded (Iacumin et al., 1997; Bocherens, 2003; Stojakowits et al., 2020, 2021). Rather, a range of environmental factors, such as humidity, temperature, and atmospheric CO_2 partial pressure affected the carbon isotope composition of the prevalent C_3 vegetation at that time, which directly affected physiological parameters controlling isotope fractionation in plant tissues (Tieszen, 1991). Decreased temperatures, a lower atmospheric CO_2 partial pressure, and increased water stress provoke increased $\delta^{13}C$ values, while high water availability, reduced light, and denser vegetation result in overall decreased $\delta^{13}C$ values (Tieszen, 1991; Pataki et al., 2003; Drucker et al., 2008; Kohn, 2010; Bonafini et al., 2013). Apart from increased lichen consumption elevated $\delta^{13}C$ values could therefore be either a response to increasing drought or to reduced vegetation cover, as exemplified for fossil reindeer (Drucker et al. 2011).

On a landscape scale, different soil moisture conditions on slope versus valley positions result in distinct $\delta^{13}C$ differences. For instance, C_3 plants growing in valleys had on average 2‰ lower $\delta^{13}C$ values than those at the slopes in an arid landscape in northwest China (Wang et al., 2005). Such small-scale differences are relevant for the local (e.g., hare) or likely non-migratory (e.g., bison, horse, ibex) mammals in our assemblage, while reindeer (Britton, 2010) and mammoth (Wooller et al., 2021) presumably migrated over greater distances and could therefore also reflect isotopic signatures of a broader geographical range. However, it is a matter of debate if reindeer migration took place in Europe in every region and at every time during the last glacial period (Fontana, 2017). For the investigated area, it can therefore be assumed that at least ibex lived in a habitat characterised by edaphically drier conditions which might have been the case on the exposed slopes and higher elevations north and northwest of the study sites (Fig. 1). In contrast, hare, horse, and bison presumably lived in habitats with edaphically more humid conditions; e.g., in valleys or river floodplains of the Danube and its tributaries south of the study sites (Fig. 1). At least for modern wild Przewalski's horses, a preference for riparian habitats in the Gobi Desert is confirmed by satellite telemetry. In contrast to Asiatic wild asses in the same region, Przewalski's horses have a much smaller home range along riparian zones, and preferred floodplain vegetation (Kaczensky et al., 2008). In addition, horses and bisons need to drink water regularly (Caboń-Raczyńska et al., 1983, 1987; Scheibe et al., 1998; Kaczensky et al., 2008). These arguments support an edaphically more humid, most likely

riparian habitat, where hares and bisons lived alongside horses during the LGM (Fig. 4b). Whether the $\delta^{13}C$ values of potentially migratory species, such as reindeer and mammoth just accidentally fall within the fields of mammals of edaphically drier (ibex) and wetter habitats (horse, hare, bison), respectively, remains to be resolved with other techniques (e.g., $^{87}Sr/^{86}Sr$; Britton et al., 2011) in the future.

Schwartz-Narbonne et al. (2015) reported that certain ecological niches can be occupied by multiple species, and despite the rather inhospitable conditions during the last glacial, these environments apparently allowed for a greater variety of habitats with options for both generalist and specialised diet. For instance, the authors report an overlap of equine $\delta^{15}N$ values with those of woolly mammoths, whereas in our study, horse, hare, and reindeer of the pre-LGM food web overlap but at the same time have broader niches than in the LGM (Fig. 6a,c), suggesting availability of more diverse food sources for these taxa during pre-LGM. This is confirmed by the pollen record from Bergsee in the Black Forest (southern Germany), which is one of the few continuous records of floral biodiversity covering the LGM in the northern Alpine foreland (Fig. 2f; Duprat-Oualid et al., 2017). During the time of KW, HU, and LK, i.e., in the latest MIS 3, the Bergsee record still shows up to 30% shrub and tree pollen, whereas the values decrease to below 20% in the LGM. This is in agreement with other palynological records that indicate small patches of trees during late MIS 3, while after 30k cal a BP arctic plant assemblages prevailed and pedogenesis came to an end (Stojakowits et al., 2021). The presence of shrubs and trees in the study area during the pre-LGM is evidenced by abundant occurrence of charcoal found in the archaeological layers at KW+HU (Neugebauer-Maresch, 2008; Händel, 2017). Wood anatomical studies on charcoal particles from KW+HU and the adjacent site Krems-Wachtberg 2005-2015 allowed the identification of predominantly pine wood with minor contributions of spruce/larch and single specimens of fir and beech wood (Einwögerer, 2000; Neugebauer-Maresch and Cichocki 2008; Cichocki et al., 2014).

In both periods, goose exhibits particularly high nitrogen isotope values among the herbivores, possibly reflecting an occupation of a particular habitat that differs from that of other herbivores. This could be connected to the uptake of a higher proportion of aquatic food or partial feeding in more southerly habitats due to seasonal migration. An accurate interpretation, however, is hardly possible due to the scarce data.

5.2 Food resources and trophic levels

$\delta^{15}N$ values of the most abundant herbivores during the pre-LGM show a large inter-taxon variability (Fig. 5a) leading to a broad niche partitioning (Fig. 6a). In contrast, niche breadth shrinks considerably during the LGM and isotopic niches cluster closer together (Fig. 6a). Most likely this is the result of a narrower range of food resources during the cold and arid LGM compared to the climatically more favourable previous periods.

Apart from hare, all other common herbivore taxa's $\delta^{15}N$ values decrease towards the LGM (Fig. 5a). Several previous studies already documented such a $\delta^{15}N$ shift at around the same time for horses, reindeer, bison, or red deer (Drucker et al., 2003; Richards and Hedges, 2003; Stevens and Hedges, 2004; Stevens et al., 2008). Our data allows further narrowing the time frame for the $\delta^{15}N$ shift to approximately the period between 29 and 24k cal a BP for Lower Austria.

At the pre-LGM sites KW+HU, $\delta^{15}N$ values of all carnivores are on average 2.8‰ higher than those of the herbivores, whereas during the LGM site KG, the average difference between carnivores and herbivores is 5.2‰, suggesting a difference of at least one trophic level and increased trophic enrichment in the LGM. In the $\delta^{13}C$-$\delta^{15}N$ space, two clusters of carnivores are observed at KW+HU (Fig. 4a): Wolf and wolverine ($\delta^{13}C$=-19.7‰, $\delta^{15}N$=8.8‰ for both) exhibit 0.5‰ higher $\delta^{13}C$ and about 1.1‰ higher $\delta^{15}N$ values than arctic and red fox ($\delta^{13}C$=-20.2‰ and $\delta^{13}C$=-20.5‰, $\delta^{15}N$=7.5 and $\delta^{15}N$=7.2‰, respectively). Assuming a trophic enrichment factor of 1.1±1.1‰ for $\delta^{13}C$ and 3.2±1.8‰ for $\delta^{15}N$ (Krajcarz et al., 2018), this results in prey values for foxes in the fields of all abundant herbivores except for ibex, reindeer, and mammoth. This may suggest that foxes at KW+HU fed mainly on carrion and small mammals like hare. Likewise, wolf and wolverine could have fed on all abundant herbivores except for hare and ibex. This is not in conflict with other studies that have inferred horses and possibly mammoth as prey items for Pleistocene wolves based on statistical analyses (Bocherens et al., 2015).

However, our dataset is biased by prehistoric human's selection and therefore lacks, e.g., micromammals that may have been an important prey item especially for foxes (Baumann et al., 2020). Red and arctic foxes are opportunistic predators that can change trophic behaviour and adapt to new diet whenever necessary (Baumann et al., 2020). Foraging on micromammals on the one hand and scavenging on large mammals (potentially even other carnivores) on the other hand could explain the high $\delta^{15}N$ variability of arctic fox in the LGM. For foxes, specialisation on micromammal prey or carrion of large herbivores was observed to cause inter-

specimen $\delta^{15}N$ differences of up to several permille at other Palaeolithic sites, too, similar as in the LGM at KG.

5.3 The special case of woolly mammoth

In some cases, altering environmental conditions may lead to changing isotopic niches of certain species, such as the woolly mammoth. In the pre-LGM food web, mammoths are exceptional as they reveal the highest $\delta^{15}N$ values of all herbivores and appear on a similar level as carnivores. This phenomenon is already known from other pre-LGM sites in Eurasia, e.g., from France (Bocherens et al., 2005; Drucker et al., 2015), north-eastern China (Ma et al., 2017, 2021), Belgium (Bocherens et al., 1997, 2001), Beringia (Bocherens et al., 1994; Fox-Dobbs et al., 2008), Germany (Bocherens et al., 2011; Drucker et al., 2015) and Yakutia (Bocherens et al., 1996; Szpak et al., 2010; Iacumin et al., 2000, 2010). These high $\delta^{15}N$ values in mammoth collagen could indicate a special diet and thus a distinct dietary niche, a particular habitat, or mammoth-specific physiological or metabolic processes. Results from compound specific isotope analyses on collagen amino acids (phenylalanine and glutamate) of Pleistocene mammoths from Yukon, Canada, showed, however, that the high $\delta^{15}N$ values of collagen come from high $\delta^{15}N$ values of the plants consumed rather than from metabolic processes (Schwartz-Narbonne et al., 2015; Naito et al., 2016). Several studies show that mammoths mainly fed on forbs and graminoids, i.e., grasses and sedges, which tend to have higher $\delta^{15}N$ values (Stewart et al., 2003; Wang and Wooller, 2006) compared to shrubs and lichen (Wang and Wooller, 2006; Finstad and Kielland, 2011; Kristensen et al., 2011). Moreover, remains of grasses and sedges were also found in teeth of fossil mammoths from Beringia (Guthrie, 2001; Drucker, 2022). A similar diet can also be reconstructed for woolly rhinoceros and steppe bison, which show $\delta^{15}N$ values partly similar to those of mammoths in the pre-LGM food web in our study (Fig. 4a) and may suggest a special dietary niche. In addition, the high $\delta^{15}N$ values in combination with the low $\delta^{13}C$ values of pre-LGM mammoth collagen could also indicate a freshwater plant food source. Kirillova et al. (2016) found considerable amounts of freshwater plants in MIS 3 mammoth faeces from northern Russia and concluded that mammoths may also have occupied freshwater, riparian, and watershed biotopes.

Our pre-LGM data imply that mammoths occupied an ecological niche where high $\delta^{15}N$ values and lower $\delta^{13}C$ values were prevalent and that was not used by other herbivores in the same extent. $\delta^{15}N$ values of plants are controlled by inorganic primary nitrogen sources (NO_3^-, NH_4^+ and N_2) in the soil as well as their respective isotope discrimination, caused by incorporation or

561 dissimilation (Högberg, 1997; Evans, 2001; Werner and Schmidt, 2002). In addition, great
562 amounts of mammoth dung may have functioned as organic fertiliser in soils which would have
563 resulted in higher $\delta^{15}N$ values of plants (Georgi et al., 2005; Bogaard et al., 2007; Fraser et al.,
564 2011) in the preferred ecological habitat of mammoths during pre-LGM time. This
565 interpretation, however, seems very unlikely for our dataset, as other herbivores do not show
566 elevated $\delta^{15}N$ values.

567 Accordingly, ecological patterns of mammoth in the pre-LGM period support both distinct
568 feeding habits and the occupation of a specific habitat that is entirely different from habitats of
569 other herbivores (exception in our study sample is a single musk ox specimen) (Fig. 4, 5).
570 Changing climate in different geographical or temporal zones towards the end of the
571 Pleistocene, however, may have led to the disappearance of such special niches and specific
572 adaptations of mammoth populations (Drucker et al., 2003; Schwartz-Narbonne et al., 2015).
573 This is in accordance with Nadachowski et al. (2018) who reported significant changes in
574 mammoth territories across Europe between 29 and 14 ka and an almost complete
575 disappearance of mammoths during the LGM around 21 to 19 ka for the Northern European
576 Plain. Drucker et al. (2018) show that the distinct ecological niche of the woolly mammoth
577 changed shortly after the LGM in Europe around 18k cal a BP. $\delta^{15}N$ values of mammoths from
578 Mezhyrich in the Eastern European Plain decreased to the level of other herbivorous species
579 and are in accordance with the mammoth nitrogen isotope values from Kammern-Grubgraben
580 in this study (Fig. 4, 5). Based on our data, however, the decline of mammoth $\delta^{15}N$ values
581 already occurred around 22k cal a BP and thus earlier than previously reported. One possible
582 cause for these changes is the climatic deterioration of the LGM that started around 30k cal a
583 BP and caused large-scale climatic and environmental changes on both global and regional
584 scales (Luetscher et al., 2015; Kämpf et al., 2022). Alternatively, pre-LGM mammoths could
585 have spent most of the time in other regions with distinctly higher isotope values of food sources
586 and just seasonally migrated into the study area. As a consequence, the pre-LGM mammoths
587 may have been more migratory than mammoths during the LGM.

588 5.4 Implications for environmental changes between the Early Gravettian and the LGM

589 In general, substantial environmental changes may lead to changes in the nitrogen isotope
590 pattern at the base of terrestrial food webs (Stevens et al., 2008; Bocherens et al., 2014;
591 Schwartz-Narbonne et al., 2015). This is evident in our study, where $\delta^{15}N$ mean values of
592 herbivores are generally lower in the LGM compared to the pre-LGM periods, except for hare

(Fig. 5a). Plant $\delta^{15}N$ values depend on various factors, such as soil $\delta^{15}N$, pedogenesis, nutrient availability, soil acidity and nitrogen cycling (Högberg, 1997; Drucker et al., 2003; Stevens and Hedges, 2004; Stevens et al., 2008). These parameters are to a great extent controlled by climate factors, which is why plant and soil $\delta^{15}N$ values indirectly correlate with climatic factors, such as mean annual precipitation and mean annual temperature (Handley et al., 1999; Amundson et al., 2003, Craine et al., 2015). The $\delta^{15}N$ values of modern soils show a latitudinal variability, where cold and/or wet ecosystems at high latitudes are the most depleted and hot and/or arid zones the most ^{15}N enriched (Amundson et al., 2003). However, $\delta^{15}N$ values of animal collagen in the last glacial may have been influenced also by temperature-induced thawing of permafrost affecting soil moisture and soil activity (Stevens et al., 2008). On the other hand, low temperatures hamper nitrogen cycling processes such as remineralisation, nitrification, and denitrification leading to lower $\delta^{15}N$ values (Drucker et al., 2003). Results similar to ours were reported by Stevens et al. (2008), who found significant changes in $\delta^{15}N$ collagen of reindeer over the last glacial period. Before 24k cal a BP, reindeer had significantly higher $\delta^{15}N$ values (mean: 4.2‰) than after 24k cal a BP, when $\delta^{15}N$ values gradually decreased (mean: 2.9‰) until 16k cal a BP, when, finally, $\delta^{15}N$ slightly increased again as conditions became wetter (Stevens et al., 2008). Higher $\delta^{15}N$ values in our study (Fig. 4, 5) would thus correspond to higher soil moisture and increased soil microbial activity during the pre-LGM compared to the LGM.

The pre-LGM sites fall into a time period with severe climatic fluctuations best known from Greenland ice core records (Fig. 2h,i,j). For instance, $\delta^{15}N$ values of air enclosed in bubbles and $\delta^{18}O$ values from ice cores of the North Greenland Ice Core Project (NGRIP) provide temperature records and are inversely correlated with Ca^{2+} records representing dust deposition (Mayewski et al., 1997; Andersen et al., 2004; Kindler et al., 2014; Rasmussen et al., 2014). The pre-LGM sites were occupied around the short-termed Greenland Interstadials (GI) 5.2 and 5.1, during which seasonal melting of continuous permafrost may have occurred. As such, a predominance of tundra gley soils has been reported for this time interval at the loess-palaeosol sequence of the Nussloch site in southern Germany (Fig. 2g; Antoine et al., 2009; Moine et al., 2017; Maier et al., 2021). At Krems-Wachtberg 2005-2015, the sediment sequence of this time interval partly shows periglacial features (Terhorst et al., 2014), which was also confirmed for the main archaeological layer AH 4 (Händel et al., 2021b). The slightly broader range of $\delta^{13}C$ values of bone collagen from this time period may also indicate an ameliorated climate, as it indicates a more diversified diet in a mosaic environment. This is in agreement with pollen data

626 from the Alpine region and the Black Forest showing a predominance of forest-tundra
627 vegetation for this time interval in contrast to the subsequent period of the LGM (Heiri et al.,
628 2014; Stojakowits et al., 2021; Kämpf et al., 2022).

629 Considering the $\delta^{15}N$ value shift as an indication of environmental and climatic changes,
630 decreased $\delta^{15}N$ collagen values from the LGM site KG would accordingly correspond to cold
631 and arid conditions as continuous permafrost prevailed and large amounts of water were stored
632 in permafrost soils and adjacent glaciated areas (Stevens et al., 2008). Low temperatures but
633 relatively stable conditions can be deduced from the NGRIP record (Fig. 2h,i,j), and loess
634 records from KG point to relatively constant environmental conditions during the main
635 occupation phase (Reiss et al., 2022). Low soil moisture, hardly any soil activity and only
636 incipient tundra gley formation in the predominantly homogeneous loess (Antoine et al., 2009)
637 are assumed for the period between 21 and 19 ka (Maier et al., 2021). Moreover, Drucker et al.
638 (2012) attributed lower $\delta^{15}N$ collagen values of reindeer, red deer, and horse to continuous
639 permafrost and/or to proximity of glacier fields, and the highest $\delta^{15}N$ collagen values to regions
640 of discontinuous permafrost.

641

642 ## 6. Conclusions

643 We compared $\delta^{13}C$ and $\delta^{15}N$ of faunal collagen from the Early Gravettian/pre-LGM sites HU,
644 KW and LK with the Early Epigravettian/LGM site KG (AH 2). Food webs from both periods
645 reveal a characteristic structure with differences in trophic ecology between herbivores and
646 carnivores. A $\delta^{13}C$ clustering between the herbivorous species hare and horse on the one hand
647 and ibex on the other hand points to niche partitioning among herbivorous groups associated
648 with distinct habitats along a local humidity gradient. During the pre-LGM, the potentially
649 migratory mammoth does not cluster in one of these groups, but in the LGM it overlaps with
650 hare, horse, and bison. Reindeer on the other hand clusters with ibex in both periods, albeit
651 being considered as migratory. These ambiguities related to the migratory behaviour of
652 mammoth and reindeer can only be resolved by applying other isotope techniques such as
653 $^{87}Sr/^{86}Sr$ in future studies.

654 The general $\delta^{15}N$ shift of 3.3‰ between all herbivores of two investigated time periods
655 (KW+HU, KG) can be attributed to climatically induced changes in the environment. This shift
656 lowers to 2.0‰ if mammoth is excluded. Previously reported, strikingly high nitrogen isotope

values of mammoths can also be confirmed for the Early Gravettian/pre-LGM sites in this study, but at the same time, we show that the disappearance of this particular niche occurred during the LGM before 23-22k cal a BP, and thus earlier than previously established for Central Europe. The isotopic niche widths expressed by SIBER analyses indicate larger habitat range for herbivores during the pre-LGM compared to the LGM, with the exception of ibex and mammoths. Accordingly, the herbivore clusters tend to increasingly overlap at the LGM site KG. As climatic conditions became more extreme in the course of the LGM, and woody plants declined, certain habitats disappeared, and different taxa had to share ecological niches. This decrease in habitats should also have resulted in a greater homogeneity of food sources as indicated by restricted isotopic ranges of non-migratory herbivores during the LGM compared to the pre-LGM period. Also, with the advances of Alpine and Baltic ice shields during the LGM, the ranges for migratory mammals, in particular mammoth, most probably became more restricted, which might have led to a greater isotopic similarity to more local mammals during the LGM.

Data availability. All relevant data is available in Table 1 and Supplementary Table S1.

Supporting information. Table S1. Summary of all isotope and elemental data.

Author contributions. LR carried out collagen extractions, evaluated and visualised the data and wrote the original draft. CM, MH, AL, AM, and KP contributed substantially to the text. KP taxonomically identified the study material from Kammern-Grubgraben and Langenlois A. HW carried out most of the stable isotope analyses. TE and MH provided the study material. All authors reviewed and approved the manuscript. CM and KP initially designed the study with contributions of AM and TE.

Competing interests. None.

Acknowledgements. We gratefully acknowledge financial support from the German Research Foundation (DFG) (grant no. MA 4235/12-1, project no. 424736737). We thank U. Simon and N. Buchinger for discussion about the site Kammern-Grubgraben. We thank N. Bova, T. Stauber, and J. Bügenburg for assistance in the isotope laboratory, C. Ehli for help with FTIR-analyses in the facility of the Institute of Physical Chemistry (FAU), and M. Häusser for support with GIS. We thank K. Britton and an anonymous reviewer for their thorough reviews and A. Brauer for editorial work.

688

689 References

690 Ambrose SH 1990. Preparation and characterization of bone and tooth collagen for isotopic
691 analysis. *Journal of Archaeological Science* **17**: 431–451.

692 Ambrose SH, Norr L. 1993. Experimental evidence for the relationship of the carbon isotope
693 ratios of whole diet and dietary protein to those of bone collagen and carbonate. In
694 *Prehistoric Human Bone, Archaeology at the Molecular Level*, Lambert J, Grupe G (eds).
695 Springer: Berlin, Heidelberg; 1–37.

696 Amundson R, Austin AT, Schuur, EA, et al. 2003. Global patterns of the isotopic composition
697 of soil and plant nitrogen. *Global Biogeochemical Cycles* **17**: 1031.

698 Andersen KK, Azuma N, Barnola JM, et al. 2004. High-resolution record of Northern
699 Hemisphere climate extending into the last interglacial period. *Nature* **431**, 147–151.

700 Andersen KK, Svensson A, Johnsen SJ, et al. 2006. The Greenland Ice Core Chronology 2005,
701 15–42 ka. Part 1: constructing the time scale. *Quaternary Science Reviews* **25**: 3246–3257.

702 Antoine P, Rousseau DD, Moine O, et al. 2009. Rapid and cyclic aeolian deposition during the
703 Last Glacial in European loess: a high-resolution record from Nussloch, Germany.
704 *Quaternary Science Reviews* **28**: 2955–2973.

705 Barnett BA. 1994. Carbon and nitrogen isotope ratios of caribou tissue, vascular plants, and
706 lichens from northern Alaska. Master's Thesis, University of Alaska, Fairbanks.

707 Baumann C, Bocherens H, Drucker DG, et al. 2020. Fox dietary ecology as a tracer of human
708 impact on Pleistocene ecosystems. *PloS ONE* **15**: e0235692.
709 https://doi.org/10.1371/journal.pone.0235692

710 Blaser PC, Kipfer R, Loosli HH, et al. 2010. A 40 ka record of temperature and permafrost
711 conditions in northwestern Europe from noble gases in the Ledo-Paniselian Aquifer
712 (Belgium). *Journal of Quaternary Science* **25**(6): 1038-1044.

713 Bocherens H. 2003. Isotopic biogeochemistry and the palaeoecology of the mammoth steppe
714 fauna. *Deinsea* **9**(1): 57–76.

715 Bocherens H, Fizet M, Mariotti A, et al. 1991. Isotopic Biogeochemistry (^{13}C, ^{15}N) of fossil
716 vertebrate collagen: implications for the study of fossil food web including Neandertal Man.
717 *Journal of Human Evolution* **20**: 481–492.

718 Bocherens H, Fizet M, Mariotti A, et al. 1994. Contribution of isotopic biogeochemistry ^{13}C,
719 ^{15}N, ^{18}O to the paleoecology of mammoths (*Mammuthus primigenius*). *Historical Biology* **7**:
720 187–202.

721 Bocherens H, Pacaud G, Lazarev P, et al. 1996. Stable isotope abundances ^{13}C, ^{15}N in collagen
722 and soft tissues from Pleistocene mammals from Yakutia. Implications for the paleobiology
723 of the mammoth steppe. *Palaeogeography, Palaeoclimatology, Palaeoecology* **126**(1/2):
724 31–44.

725 Bocherens H, Billiou D, Patou-Mathis M, et al. 1997. Isotopic biogeochemistry (^{13}C, ^{15}N) of
726 fossil mammal collagen from Scladina cave (Sclayn, Belgium). *Quaternary Research* **48**:
727 370–380.

728 Bocherens H, Toussaint M, Billiou D, et al. 2001. New isotopic evidence for dietary habits of
729 Neandertals from Belgium. *Journal of Human Evolution* **40**: 497–505.

730 Bocherens H, Drucker D. 2003. Trophic level isotopic enrichment of carbon and nitrogen in
731 bone collagen: Case studies from recent and ancient terrestrial ecosystems. *International*
732 *Journal of Osteoarchaeology* **13**: 46–53.

733 Bocherens H, Drucker DG, Billiou D, et al. 2005. Isotopic evidence for diet and subsistence
734 pattern of the Saint-Césaire I Neanderthal: review and use of a multi-source mixing model.
735 *Journal of Human Evolution* **49**: 71–87.

736 Bocherens H, Drucker DG, Bonjean D, et al. 2011. Isotopic evidence for dietary ecology of
737 cave lion (Panthera spelaea) in North-Western Europe: Prey choice, competition and
738 implications for extinction. *Quaternary International* **245**: 249–261.

739 Bocherens H, Drucker DG, Madelaine S. 2014. Evidence for a ^{15}N positive excursion in
740 terrestrial foodwebs at the middle to upper Palaeolithic transition in South-western France:
741 implication for early modern human palaeodiet and palaeoenvironment. *Journal of Human*
742 *Evolution* **69**: 31–43.

743 Bocherens H, Drucker DG, Germonpré M, et al. 2015. Reconstruction of the Gravettian food-
744 web at Předmostí I using multi-isotopic tracking ^{13}C, ^{15}N, ^{34}S of bone collagen. *Quaternary*
745 *International* **359-360**: 211–228.

746 Boogard A, Heaton TH, Poulton P, et al. 2007. The impact of manuring on nitrogen isotope
747 ratios in cereals: archaeological implications for reconstruction of diet and crop management
748 practices. *Journal of Archaeological Science* **34**(3): 335–343.

749 Bonafini M, Pellegrini M, Ditchfield P, et al. 2013. Investigation of the 'canopy effect' in the
750 isotope ecology of temperate woodlands. *Journal of Archaeological Science* **40**(11): 3926–
751 3935.

752 Bösl C, Grupe G, Peters J. 2006. A Late Neolithic vertebrate food web based on stable isotope
753 analyses. *International Journal of Osteoarchaeology* **16**: 296–315.

754 Brandtner F. 1990. Die Paläolithstation "Grubgraben" bei Kammern. Vorläufige Ergebnisse
755 neuerer Grabungen. *Fundberichte aus Österreich* **28**(1989): 17–26.

756 Brandtner F. 1996. Zur geostratigraphischen und kulturellen Zuordnung der Paläolithstation
757 Grubgraben bei Kammern, NÖ. In *Paleolithic in the Middle Danube Region*, Svoboda J (ed).
758 Festschrift for B. Klíma, Dolní Věstonice Studies 4: Brno; 121–146.

759 Britton K. 2010. Multi-isotope analysis and the reconstruction of prey species palaeomigrations
760 and palaeoecology. Doctoral dissertation, Durham University.

761 Britton K., Grimes V, Niven L, et al. 2011. Strontium isotope evidence for migration in late
762 Pleistocene Rangifer: Implications for Neanderthal hunting strategies at the Middle
763 Palaeolithic site of Jonzac, France. *Journal of Human Evolution* **61**(2): 176–185.

764 Britton K, Gaudzinski-Windheuser S, Roebroeks W, et al. 2012. Stable isotope analysis of well-
765 preserved 120,000-year-old herbivore bone collagen from the Middle Palaeolithic site of
766 Neumark-Nord 2, Germany reveals niche separation between bovids and equids.
767 *Palaeogeography, Palaeoclimatology, Palaeoecology* **333-334**: 168–177.

768 Brock F, Higham T, Ramsey C. 2010. Pre-screening techniques for identification of samples
769 suitable for radiocarbon dating of poorly preserved bones. *Journal of Archaeological*
770 *Science* **37**: 855–865.

771 Bronk Ramsey C. 2009. Bayesian analysis of radiocarbon dates. *Radiocarbon* **51**(1): 337–360.

772 Caboń-Raczyńska K, Krasińska M, Krasiński Z. 1983. Behaviour and daily activity rhythm of
773 European bison in winter. *Acta Theriologica* **28**(18): 273–299.

774 Caboń-Raczyńska K, Krasińska M, Krasiński ZA, et al. 1987. Bisoniana XCVII. Rhythm of
775 daily activity and behavior of European bison in the Białowieża Forest in the period without
776 snow cover. *Acta Theriologica*, **32**(21): 335–372.

777 Cersoy S, Zazzo A, Lebon M, et al. 2016. Collagen extraction and stable isotope analysis of
778 small vertebrate bones: a comparative approach. *Radiocarbon* **59**: 679–694.
779 https://doi.org/10.1017/RDC.2016.82

780 Cichocki O, Knibbe B, Tillich I. 2014. Archaeological significance of the Palaeolithic charcoal
781 assemblage from Krems-Wachtberg. *Quaternary International* **351**: 163–171.

782 Coplen TB. 2011. Guidelines and recommended terms for expression of stable-isotope-ratio
783 and gas-ratio measurement results. *Rapid Communications in Mass Spectrometry* **25**: 2538–
784 2560.

785 Coltrain JB, Harris JM, Cerling TE, et al. 2004. Rancho La Brea stable isotope biochemistry
786 and its implications for the palaeoecology of the late Pleistocene, coastal southern California.
787 *Palaeogeography, Palaeoclimatology, Palaeoecology* **205**: 199–219.

788 Craine JM, Elmore AJ, Wang L, et al. 2015. Convergence of soil nitrogen isotopes across global
789 climate gradients. *Scientific Reports* **5**: 8280. https://doi.org/10.1038/srep08280

790 Delisle G, Grassmann S, Cramer B, et al. 2007. Estimating episodic permafrost development
791 in northern Germany during the Pleistocene. In: *Sedimentary Processes and Products*, Part
792 3 *Quaternary Glacial Systems*, Hambrey MJ, Christoffersen P, Glasser NF, et al. (eds).
793 International Association of Sedimentologists, Blackwell Publishing Ltd: Malden, Oxford,
794 Victoria: 109-119.

795 DeNiro MJ. 1985. Postmortem preservation and alteration of in vivo bone collagen isotope
796 ratios in relation to palaeodietary reconstruction. *Nature* **317**: 806–809.

797 DeNiro MJ, Epstein S. 1978. Influence of diet on the distribution of carbon isotopes in animals.
798 *Geochimica et Cosmochimica Acta* **42**: 495–506. https://doi.org/10.1016/0016-
799 70377890199-0

DeNiro MJ, Epstein S. 1981. Influence of diet on the distribution of nitrogen isotopes in animals. *Geochimica et Cosmochimica Acta* **45**: 341–351. https://doi.org/10.1016/0016-70378190244-1

DeNiro MJ, Weiner S. 1988. Chemical, enzymatic and spectroscopic characterization of "collagen" and other organic fractions from prehistoric bones. *Geochimica et Cosmochimica Acta* **52**: 2197–2206.

Dobberstein RC, Collins MJ, Craig OE, et al. 2009. Archaeological collagen: Why worry about collagen diagenesis? *Archaeological and Anthropological Sciences* **1**: 31–42. https://doi.org/10.1007/s12520-009-0002-7

Drucker DG. 2022. The isotopic ecology of the mammoth steppe. *Annual Review of Earth and Planetary Sciences* **50**: 395–418.

Drucker D, Bocherens H, Cleyet-Merle JJ, et al. 2000. Implications paléoenvironnementales de l'étude isotopique (^{13}C, ^{15}N) de la faune de grands mammifères des Jamblancs (Dordogne, France). *Paléo* **12**: 29–53.

Drucker DG, Bocherens H, Pike-Tay A, et al. 2001. Isotopic tracking of seasonal dietary change in dentine collagen: preliminary data from modern caribou. *Comptes Rendus de l'Académie des Sciences, Série II, Paris* **333**: 303–309.

Drucker DG, Bocherens H, Billiou D. 2003. Evidence for shifting environmental conditions in Southwestern France from 33,000 to 15,000 years ago derived from carbon-13 and nitrogen-15 natural abundances in collagen of large herbivores. *Earth and Planetary Science Letters* **216**: 163–173.

Drucker DG, Henry-Gambier D. 2005. Determination of the dietary habits of a Magdalenian woman from Saint-Germain-la-Rivière in southwestern France using stable isotopes. *Journal of Human Evolution* **49**: 19–35.

Drucker DG, Bridault A, Hobson KA, et al. 2008. Can carbon-13 abundances in large herbivores track canopy effect in temperate and boreal ecosystems? Evidence from modern and ancient ungulates. *Palaeogeography, Palaeoclimatology, Palaeoecology* **266**: 69–82.

Drucker DG, Kind CJ, Stephan E. 2011. Chronological and ecological information on Late-glacial and early Holocene reindeer from northwest Europe using radiocarbon (^{14}C) and

stable isotope (^{13}C, ^{15}N) analysis of bone collagen: Case study in southwestern Germany. *Quaternary International* **245**: 218–224.

Drucker DG, Bridault A, Cupillard C. 2012. Environmental context of the Magdalenian settlement in the Jura Mountains using stable isotope tracking (^{13}C, ^{15}N, ^{34}S) of bone collagen from reindeer (*Rangifer tarandus*). *Quaternary International* **272-273**: 322–332.

Drucker DG, Vercoutère C, Chiotti L, et al. 2015. Tracking possible decline of woolly mammoth during the Gravettian in the Dordogne and the Swabian Jura using multi-isotope tracking (^{13}C, ^{14}C, ^{15}N, ^{34}S, ^{18}O). *Quaternary International* **359-360**: 304–317.

Drucker DG, Stevens RE, Germonpré M, et al. 2018. Collagen stable isotopes provide insight into the end of the mammoth steppe in the central East European plains during the Epigravettian. *Quaternary Research* **90**: 457–469.

Duprat-Oualid F, Rius D, Bégeot C, et al. 2017. Vegetation response to abrupt climatic changes in Western Europe from 45 to 14.7k cal a BP: the Bergsee lacustrine record (Black Forest, Germany). *Journal of Quaternary Science* **32**(7): 1008–1021.

Dytham C. 2011. Choosing and using Statistics. A biologist's guide. Third Edition. Wiley Blackwell: West Sussex.

Einwögerer T. 2000. Die jungpaläolithische Station auf dem Wachtberg in Krems, NÖ. Eine Rekonstruktion und wissenschaftliche Darlegung der Grabung von J. Bayer aus dem Jahre 1930. Mitteilungen der Prähistorischen Kommission **34**, Wien.

Einwögerer T, Händel M, Neugebauer-Maresch C, et al. 2009. ^{14}C dating of the Upper Palaeolithic site at Krems-Wachtberg, Austria. *Radiocarbon* **51**: 847–855.

Einwögerer T. 2019. Langenlois Fundstelle A. Verlag der Österreichischen Akademie der Wissenschaften **88**, pp. 206.

Evans RD. 2001. Physiological mechanisms influencing plant nitrogen isotope composition. *Trends in Plant Science* **6**(3): 121–126.

Farquhar GD, Ehleringer JR, Hubick KT. 1989. Carbon isotope discrimination and photosynthesis. *Annual Review of Plant Biology* **40**(1): 503–537.

Fedosenko AK, Blank DA. 2001. Capra sibirica. *Mammalian Species* **675**: 1–13.

857 Finstad GL, Kielland K. 2011. Landscape variation in diet and productivity of reindeer in
858 Alaska based on stable isotope analyses. *Artic, Antarctic and Alpine Research* **43**(4): 543–
859 554.

860 Fizet M, Mariotti A, Bocherens H, et al. 1995. Effect of diet, physiology and climate on carbon
861 and nitrogen isotopes of collagen in a late Pleistocene anthropic paleoecosystem France,
862 Charente, Marillac. *Journal of Archaeological Science* **22**: 67–79.

863 Fladerer FA. 2001. Die Faunareste vom jungpaläolithischen Lagerplatz Krems-Wachtberg,
864 Ausgrabung 1930: Jagdwild und Tierkörpernutzung an der Donau vor 27000 Jahren. Verlag
865 der Österreichischen Akademie der Wissenschaften.

866 Fladerer FA, Salcher-Jedrasiak T. 2008. Krems-Hundssteig 2000-2002: Archäozoologische
867 und taphonomische Untersuchungen. In *Krems-Hundssteig – Mammutjäger der Eiszeit. Ein*
868 *Nutzungsareal paläolithischer Jäger- und Sammlerinnen vor 41.000-27.000 Jahren*,
869 Neugebauer-Maresch C (ed). Mitteilungen der Prähistorischen Kommission: Wien; 67: 216–
870 312.

871 Fontana L. 2017. The four seasons of reindeer: Non-migrating reindeer in the Dordogne region
872 (France) between 30 and 18k? Data from the Middle and Upper Magdalenian at La
873 Madeleine and methods of seasonality determination. *Journal of Archaeological Science:*
874 *Reports* **12**: 346–362.

875 Fox-Dobbs K, Bump JK, Peterson RO, et al. 2007. Carnivore-specific stable isotope variables
876 and variation in the foraging ecology of modern and ancient wolf populations: case studies
877 from Isle Royale, Minnesota, and La Brea. *Canadian Journal of Zoology* **85**: 458–471.

878 Fox-Dobbs K, Leonard JA, Koch PL. 2008. Pleistocene megafauna from eastern Beringia:
879 paleoecological and paleoenvironmental interpretations of stable carbon and nitrogen
880 isotope and radiocarbon records. *Palaeogeogprahy, Palaeoclimatology, Palaeoecology* **261**:
881 30–46.

882 Fraser RA, Bogaard A, Heaton T, et al. 2011. Manuring and stable nitrogen isotope ratios in
883 cereals and pulses: towards a new archaeobotanical approach to the inference of land use
884 and dietary practices. *Journal of Archaeological Science* **38**(10): 2790–2804.

885 Georgi M, Voerkelius S, Rossmann A, et al. 2005. Multielement isotope ratios of vegetables
886 from integrated and organic production. *Plant and Soil* **275**: 93–100.

887 Germonpré M, Sablin MV, Stevens RE, et al. 2009. Fossil dogs and wolves from Palaeolithic
888 sites in Belgium, the Ukraine and Russia: osteometry, ancient DNA and stable isotopes.
889 *Journal of Archaeological Science* **36**: 473–490.

890 Gilot E. 1997. Index général des dates LV. Laboratoire du Carbone 14 de Louvain/Louvain-la-
891 Neuve. Studia Praehistorica Belgica **7**, Liége.

892 Grupe G, Mikic Z, Peters J, et al. 2003. Vertebrate food webs and subsistence strategies of
893 Meso- and Neolithic populations of central Europe, *Documenta Archaeobiologia* **1**: 193–
894 213.

895 Guiry EJ, Szpak P. 2021. Improved quality control citeria for stable carbon and nitrogen isotope
896 measurements of ancient bone collagen. *Journal of Archaeological Science* **132**: 105416.

897 Guthrie RD. 1982. Mammals of the mammoth steppe as paleoenvironmental indicators. In
898 *Paleoecology of Beringia*, Moody Hopkins D (ed). Academic: New York; 307–326.

899 Guthrie RD. 2001. Origins and causes of the mammoth steppe: a story of cloud cover, woolly
900 mammal tooth pits, buckles, and inside-out Beringia. *Quaternary Science Reviews* **20**(1-3):
901 549–574.

902 Haesaerts P. 1990. Stratigraphy of the Grubgraben Loess Sequence. In *The Epigravettian site*
903 *of Grubgraben, Lower Austria: The 1986 and 1987 excavations*, Montet-White A. (ed.).
904 ERAUL: Université de Liège, Liège; **40**: 15-35.

905 Haesaerts P, Damblon F, Neugebauer-Maresch C, Einwögerer T. 2016. Radiocarbon
906 Chronology of the Late Palaeolithic Loess Site of Kammern-Grubgraben (Lower Austria).
907 *Archaeologia Austriaca* **100**: 271–277.

908 Handley LL, Austin AT, Stewart GR, et al. 1999. The ^{15}N natural abundance ($\delta^{15}N$) of
909 ecosystem samples reflects measures of water availability. *Australian Journal of Plant*
910 *Physiology* **26**(2): 185–199.

911 Händel M. 2017. The stratigraphy of the Gravettian sites at Krems. *Quartär* **64**: 129–155.

912 Händel M, Simon U, Maier A, et al. 2021a. Kammern-Grubgraben revisited – First results from
913 renewed investigations at a well-known LGM site in east Austria, *Quaternary International*
914 **587–588**: 137–157. https://doi.org/10.1016/j.quaint.2020.06.012

915 Händel M, Thomas R, Sprafke T, et al. 2021b. Using archaeological data and sediment
916 parameters to review the formation of the Gravettian layers at Krems-Wachtberg. *Journal of*
917 *Quaternary Science* **36**(8): 1397–1413.

918 Hedges RE, Clement JG, Thomas CDL, et al. 2007. Collagen turnover in the adult femoral mid-
919 shaft: Modeled from anthropogenic radiocarbon tracer measurements. *American Journal of*
920 *Physical Anthropology* **133**(2): 808–816.

921 Heinrich W. 1973. Das Jungpalaolithikum in Niederosterreich. Unpublished dissertation,
922 University of Salzburg.

923 Heiri O, Koinig KA, Spötl C, et al. 2014. Palaeoclimate records 60-8 ka in the Austrian ans
924 Swiss Alps and their forelands. *Quaternary Science Reviews* **106**: 186–205.

925 Hobson KA. 1999. Tracing origins and migration of wildlife using stable isotopes: a review.
926 *Oecologia* **120**: 314–326.

927 Högberg P. 1997. ^{15}N natural abundance in soil-plant systems. *New Phytologist* **137**(2): 179–
928 203.

929 Hoke N, Rott A, Johler S, et al. 2019. How bone degradation, age, and collagen extraction
930 methods affect stable isotope analysis. *Archaeological and Anthropological Sciences* **11**:
931 3357–3374.

932 Iacumin P, Bocherens H, Huertas AD, et al. 1997. A stable isotope study of fossil mammal
933 remains from the Paglicci cave, Southern Italy. N and C as palaeoenvironmental indicators.
934 *Earth and Planetary Science Letters* **148**(1-2): 349–357.

935 Iacumin P, Nikolaev V, Ramigni M. 2000. C and N stable isotope measurements on Eurasian
936 fossil mammals, 40 000 to 10 000 years BP: Herbivore physiologies and
937 palaeoenvironmental reconstruction. *Palaeogeography, Palaeoclimatology, Palaeoecology*
938 **163**: 33–47.

939 Iacumin P, Davanzo S, Nikolaev V. 2006. Spatial and temporal variations in the $^{13}C/^{12}C$ and
940 $^{15}N/^{14}N$ ratios of mammoth hairs: Palaeodiet and palaeoclimatic implications. *Chemical*
941 *Geology* **231**: 16–25.

Iacumin P, Di Matteo A, Nikolaev V, et al. 2010. Climate information from C, N and O stable isotope analyses of mammoth bones from northern Siberia. *Quaternary International* **212**(2): 206–212.

Jackson AL, Inger R, Parnell AC, et al. 2011. Comparing isotopic niche widths among and within communities: SIBER – Stable Isotope Bayesian Ellipses in R. *Journal of Animal Ecology* **80**: 595–602.

Kaczensky P, Ganbaatar O, von Wehdren H, et al. 2008. Resource selection by sympatric wild equids in the Mongolian Gobi. *Journal of Applied Ecology* **45**: 1762–1769.

Kämpf L, Rius D, Duprat-.Oualid F, et al. 2022. Evidence for wind patterns and associated landscape response in Western Europe between 46 and 16 ka cal. BP. *Quaternary Science Reviews* **298**: 107846.

Kindler P, Guillevic M, Baumgartner M, et al. 2014. Temperature reconstruction from 10 to 120 kyr b2k from the NGRIP ice core. *Climate of the Past* **10**(2): 887–902.

Kirillova IV, Argant J, Lapteva EG, et al. 2016. The diet and environment of mammoths in North-East Russia reconstructed from the contents of their feces. *Quaternary International Part B* **406**: 147–161.

Kohn MJ. 2010. Carbon isotope compositions of terrestrial C_3 plants as indicators of (paleo)ecology and (paleo)climate. *PNAS* **107**(46): 19691–19695.

Krajcarz M, Pacher M, Krajcarz MT, et al. 2016. Isotopic variability of cave bears ($\delta^{15}N$, $\delta^{13}C$) across Europe during MIS 3. *Quaternary Science Reviews* **131**: 51–72.

Krajcarz MT, Krajcarz M, Bocherens H. 2018. Collagen-to-collagen prey-predator isotopic enrichment ($\Delta^{13}C$, $\Delta^{15}N$) in terrestrial mammals – a case study of subfossil red fox den. *Palaeogeography, Palaeoclimatology, Palaeoecology* **490**: 563–570.

Kristensen DK, Kristensen E, Forchhammer MC, et al. 2011. Arctic herbivore diet can be inferred from stable carbon and nitrogen isotopes in C_3 plants, faeces, and wool. *Canadian Journal of Zoology* **89**(10): 892–899.

Kronfeld-Schor N, Shargal E, Haim A, et al. 2001. Temporal partitioning among diurnally and nocturnally active desert spiny mice: Energy and water turnover costs. *Journal of Thermal Biology* **26**: 139–142.

971 Lambert JB, Shurvell HF, Lightner DA, et al. 1998. Organic structural spectroscopy. Pearson
972 College Division.

973 Lebon M, Reiche I, Gallet X, et al. 2016. Rapid quantification of bone collagen content by
974 ATR-FTIR spectroscopy. *Radiocarbon* **58**: 131–145.

975 Luetscher M, Boch R, Sodemann H, et al. 2015. North Atlantic storm track changes during the
976 last glacial maximum recorded by alpine speleothems. *Nature Communications* **6**: 6344.

977 Ma J, Fengli Z, Yuan W, et al. 2017. Tracking the foraging behavior of *Mammuthus primigenius*
978 from the late Pleistocene of northeast China, using stable isotope analysis. *Quaternary*
979 *Science* **37**(4): 885–894.

980 Ma J, Wang Y, Baryshnikov GF, et al. 2021. The *Mammuthus-Coelodonta* Faunal Complex at
981 its southeastern limit: a biogeochemical paleoecology investigation in Northeast Asia.
982 *Quaternary International* **591**: 93–106.

983 Maier A, Stojakowits P, Mayr C, et al. 2021. Cultural evolution and environmental change in
984 Central Europe between 40 and 15 ka. *Quaternary International* **581-582**: 225–240.

985 Mayewski PA, Meeker LD, Twickler MS, et al. 1997. Major features and forcing of high-
986 latitude northern hemisphere atmospheric circulation using a 110,000-year long
987 glaciochemical series. *Journal of Geophysical Research-Oceans* **102**: 26345–26366.

988 Mix AC, Bard E, Schneider R, 2001. Environmental processes of the ice age: land, oceans,
989 glaciers (EPILOG). *Quaternary Science Reviews* **20**(4): 627–657.

990 Moine O, Antoine P, Hatté C, et al. 2017. The impact of Last Glacial climate variability in west-
991 European loess revealed by radiocarbon dating of fossil earthworm granules. *PNAS* **114**(24):
992 6209–6214.

993 Montet-White A. 1988. Recent excavations at Grubgraben. A Gravettian site in Lower Austria.
994 *Archäologisches Korrespondenzblatt* **18**: 213–218.

995 Montet-White A. 1990. The Epigravettian Site of Grubgraben, Lower Austria: the 1986 and
996 1987 Excavations. *ERAUL Études et Recherche Archéologiques de l´Université de Liège* 40,
997 Liège.

998 Munizzi JS. 2017. Rethinking Holocene ecological relationships among caribou, muskoxen,
999 and human hunters on Banks Island, NWT, Canada: a stable isotope approach. PhD
1000 Dissertation, University of Western Ontario: London, Ontario, Canada.

1001 Nadachowski A, Lipecki G, Baca M, et al. 2018. Impact of climate and humans on the range of
1002 the woolly mammoth (*Mammuthus primigenius*) in Europe during MIS 2. *Quaternary*
1003 *Research* **90**: 439–456.

1004 Nadelhoffer K, Shaver G, Fry B, et al. 1996. ^{15}N natural abundances and N use by tundra plants.
1005 *Oecologia* **107**(3): 386–394.

1006 Naito YI, Drucker DG, Chikaraishi Y, et al. 2016. Ecological niche of Neanderthals from Spy
1007 Cave revealed by nitrogen isotopes of individual amino acids in collagen. *Journal of Human*
1008 *Evolution* **93**: 82–90.

1009 Neugebauer-Maresch C, Peticzka R, Frank C, et al. 2008. Stratigraphie und Befunde. In *Krems-*
1010 *Hundssteig – Mammutjägerlager der Eiszeit. Ein Nutzungsareal paläolithischer Jager- und*
1011 *Sammler(-innen) vor 41.000-27.000 Jahren*, Neugebauer-Maresch, C. (ed.). Mitteilungen
1012 der Prähistorischen: Wien; 67: 68–146.

1013 Neugebauer-Maresch C, Cichocki O. 2008. Holzbefunde. In *Krems-Hundssteig*
1014 *– Mammutjägerlager der Eiszeit. Ein Nutzungsareal paläolithischer Jager- und Sammler(-*
1015 *innen) vor 41.000-27.000 Jahren*, Neugebauer-Maresch, C. (ed.). Mitteilungen der
1016 Prähistorischen: Wien; 67: 147–167.

1017 Neugebauer-Maresch C, Stadler, P. 2008. Absolute Datierung. In *Krems-Hundssteig*
1018 *– Mammutjägerlager der Eiszeit. Ein Nutzungsareal paläolithischer Jager- und Sammler(-*
1019 *innen) vor 41.000-27.000 Jahren*, Neugebauer-Maresch, C. (ed.). Mitteilungen der
1020 Prähistorischen: Wien; 67: 168–176.

1021 Neugebauer-Maresch C, Einwögerer T, Richter J, et al. 2016. Kammern-Grubgraben. Neue
1022 Erkenntnisse zu den Grabungen 1989–1994. *Archaeologia Austriaca* **100**: 225–254.
1023 https://doi.org/10.1553/archaeologia100s225

1024 Obermaier H. 1908. Die am Wagram Durchbruch des Kamp gelegenen niederösterreichischen
1025 Quartärfundplätze. *Jahrbuch für Altertumskunde* **2**: 49–85.

1026 Parrini F, Cain III JW, Krausman PR. 2009. *Capra ibex* (Artiodactyla: Bovidae). *Mammalian*
1027 *Species* **830**: 1–12.

Pataki DE, Ehleringer JR, Flanagan LB, et al. 2003. The application and interpretation of Keeling plots in terrestrial carbon cycle research. *Global biochemical cycles* **17**(1): 1022. https://doi.org/10.1029/2001GB001850

Pfeifer S, Pasda K, Händel M et al. accepted. The osseous industry of the LGM site Kammern-Grubgraben (Lower Austria), excavations 1985-1994, and its position within the European Late Upper Palaeolithic. *Quartär*.

Rasmussen SO, Bigler M, Blockley SP, et al. 2014. A stratigraphic framework for abrupt climatic changes during the Last Glacial period based on three synchronized Greenland ice-core records: refining and extending the INTIMATE event stratigraphy. *Quaternary Science Reviews* **106**: 14–28.

Reimer PJ, Austin WEN, Bard E, et al. 2020. The IntCal20 Northern Hemisphere Radiocarbon Age Calibration Curve (0–55 cal kBP). *Radiocarbon* **62**: 725–757.

Reiss L, Stüwe C, Einwögerer T, et al. 2022. Evaluation of geochemical proxies and radiocarbon data from a loess record of the Upper Palaeolithic site Kammern-Grubgraben, Lower Austria. *E&G Quaternary Science Journal* **71**: 23–43.

Řičánková VP, Robovský J, Riegert J, et al. 2015. Regional patterns of postglacial changes in the Palearctic mammalian diversity indicate retreat to Siberian steppes rather than extinction. *Scientific Reports* **5**: 12682. https://doi.org/10.1038/srep12682

Richards MP, Hedges REM. 2003. Variations in bone collagen $\delta^{13}C$ and $\delta^{15}N$ values of fauna from Northwest Europe over the last 40000 years. *Palaeogeography, Palaeoclimatology, Palaeoecology* **193**: 261–267.

Scheibe KM, Eichhorn K, Kalz B, et al. 1998. Water consumption and watering behavior of przewalski horses (*Equus ferus przewalskii*) in a semireserve. *Zoo Biology* **17**: 181–192.

Schoeninger MJ, DeNiro MJ. 1984. Nitrogen and carbon isotopic composition of bone collagen from marine and terrestrial animals. *Geochimica et Cosmochimica Acta* **48**: 625–639.

Schwartz-Narbonne R, Longstaffe FJ, Metcalfe JZ, et al. 2015. Solving the woolly mammoth conundrum: amino acid ^{15}N-enrichment suggests a distinct forage or habitat. *Scientific Reports* **5**(1): 9791.

Schwartz-Narbonne R, Longstaffe FJ, Kardynal KJ, et al. 2019. Reframing the mammoth steppe: insights from analysis of isotopic niches. *Quaternary Science Reviews* **215**: 1–21.

Stevens RE, Hedges REM. 2004. Carbon and nitrogen stable isotope analysis of northwest European horse bone and tooth collagen, 40,000 BP-present: palaeoclimatic interpretations. *Quaternary Science Reviews* **23**(7–8): 977–991.

Stevens RE, Jacobi R, Street M, et al. 2008. Nitrogen isotope analyses of reindeer (*Rangifer tarandus*), 45,000 BP to 9,000 BP: palaeoenvironmental reconstructions. *Palaeogeography Palaeoclimatology Palaeoecology* **262**(1–2): 32–45.

Stevens RE, O'Connell TC, Hedges REM, et al. 2009. Radiocarbon and stable isotope investigations at the Central Rhineland sites of Gönnersdorf and Andernach-Martinsberg, Germany. *Journal of Human Evolution* **57**: 131–148.

Stewart KM, Bowyer T, Kie JG, et al. 2003. Niche partitioning among mule deer, elk, and cattle: Do stable isotopes reflect dietary niche? *ÉCOSCIENCE* **10**(3): 297–302.

Stojakowits P, Mayr C, Lücke A, et al. 2020. Impact of climatic extremes on Alpine ecosystems during MIS 3. *Quaternary Science Reviews* **239**: 106333. https://doi.org/10.1016/j.quascirev.2020.

Stojakowits P, Mayr C, Ivy-Ochs S, et al. 2021. Environments at the MIS 3/2 transition in the northern Alps and their foreland. *Quaternary International* **581-582**: 99–113.

Sprafke T, Schulte P, Meyer-Heintze S, et al. 2020. Paleoenvironments from robust loess stratigraphy using high-resolution color and grain-size data of the last glacial Krems-Wachtberg record (NE Austria). *Quaternary Science Reviews* **248**: 106602. https://doi.org/10.1016/j.quascirev.2020.106602.

Spöttl I. 1890. Resultate der Ausgrabungen für die Anthropologische Gesellschaft in NÖ und in Mähren im Jahre 1889. *Mitteilungen der Anthropologischen Gesellschaft Wien* XX.

Szpak P, Gröcke DR, Debruyne R, et al. 2010. Regional differences in bone collagen $\delta^{13}C$ and $\delta^{15}N$ of Pleistocene mammoths: implications for paleoecology of the mammoth steppe. *Palaeogeography, Palaeoclimatology, Palaeoecology* **286**(1-2): 88–96.

1083 Terhorst B, Kühn P, Damm B, et al. 2014. Paleoenvironmental fluctuations as recorded in the
1084 loess-paleosol sequence of the Upper Paleolithic site Krems-Wachtberg. *Quaternary*
1085 *International* **351**: 67–82.

1086 Tieszen LL. 1991. Natural variations in the carbon isotope values of plants: implications for
1087 archaeology, ecology, and paleoecology. *Journal of Archaeological Science* **18**: 227–248.

1088 Vandenberghe J, French HM, Gorbunov A, et al. 2014. The Last Permafrost Maximum (LPM)
1089 map of the Northern Hemisphere: permafrost extent and mean annual air temperatures, 25–
1090 17 ka BP. *Boreas* **43**: 652-666.

1091 van Klinken GJ. 1999. Bone collagen quality indicators for palaeodieatary and radiocarbon
1092 measurements. *Journal of Archaeological Science* **26**: 687–695.

1093 Voelker AHL, workshop participants. 2002. Global distribution of centennial-scale records for
1094 Marine Isotope Stage (MIS) 3: a database. *Quaternary Science Reviews* **21**: 1185–1212.

1095 Wang Y, Wooller MJ. 2006. The stable isotopic (C and N) composition of modern plants and
1096 lichens from northern Iceland: with ecological and paleoenvironmental implications. *Jökull*
1097 **56**: 27–38.

1098 Wang G, Han J, Zhou L, et al. 2005. Carbon isotope ratios of plants and occurrences of C_4
1099 species under different soil moisture regimes in arid region of Northwest China. *Physiologia*
1100 *Plantarum* **125**: 74–81.

1101 Werner RA, Schmidt HL. 2002. The in vivo nitrogen isotope discrimination among organic
1102 plant compounds. *Phytochemistry* **61**: 465–484.

1103 Wooller MJ, Bataille C, Druckenmiller P, et al. 2021. Lifetime mobilityx of an Arctic woolly
1104 mammoth. *Science* **373**(6556): 806-808.

1105 Yeakel JD, Guimarães Jr. PR, Bocherens H, et al. 2013. The impact of climate change on the
1106 structure of Pleistocene food webs across the mammoth steppe. *Proceedings of the Royal*
1107 *Society B: Biological Sciences* **280**: 20130239.

1108 Zimov SA, Chuprynin VI, Oreshko AP, et al. 1995. Steppe-tundra transition: a herbivore-driven
1109 biome shift at the end of the Pleistocene. *The American Naturalist* **146**(5): 765–794.

1110 Zimov SA, Zimov NS, Tikhonov AN, et al. 2012. Mammoth steppe: a high productive
1111 phenomenon. *Quaternary Science Reviews* **57**: 26–45.

1112 **Table 1.** List of species and analysed material sampled from Krems-Hundssteig 2000-2002, Krems-Wachtberg 1930, Langenlois A, and Kammern-
1113 Grubgraben with indication of the find layer and the minimum number of individuals (MNI) in the respective sites.

Study site	Sample ID	Species	Skeletal element	Material	Side	Age	Find layer	MNI
Krems-Hundssteig 2000-2022	HU-100/1	hare *(Lepus* sp.*)*		bone			3.44	
Krems-Hundssteig 2000-2002	HU-168/3	hare *(Lepus* sp.*)*		bone			3.44	2
Krems-Hundssteig 2000-2002	HU-253/5	hare *(Lepus* sp.*)*	Mandibula	bone	right		3.24	
Krems-Hundssteig 2000-2002	HU-276/5	horse *(Equus* sp.*)*		bone			3.44	
Krems-Hundssteig 2000-2002	HU-201/15	horse *(Equus* sp.*)*		bone			3.24	3
Krems-Hundssteig 2000-2002	HU-33/4	horse *(Equus* sp.*)*	Maxilla P2	tooth	left		3.21	
Krems-Hundssteig 2000-2002	HU-158/3	ibex *(Capra ibex)*	Metacarpus III/IV	bone	left		3.24	1
Krems-Hundssteig 2000-2002	HU-159/2	arctic fox *(Vulpes lagopus)*	Mandibula	bone	left		3.44	1
Krems-Hundssteig 2000-2002	HU-165/1	red deer *(Cervus elaphus)*	Calcaneus	bone			3.44	
Krems-Hundssteig 2000-2002	HU-372/24	red deer *(Cervus elaphus)*	Mandibula	bone			3.22	2
Krems-Hundssteig 2000-2002	HU-206/2,3	red deer *(Cervus elaphus)*	Carpale	bone			3.24	
Krems-Hundssteig 2000-2002	HU-156/2	red fox *(Vulpes vulpes)*	Cranium	bone			3.44	
Krems-Hundssteig 2000-2002	HU-432/1	red fox *(Vulpes vulpes)*	Cranium, P4 und M1	tooth			3.23	2
Krems-Hundssteig 2000-2002	HU-196/3	reindeer *(Rangifer tarandus)*	Radius	bone	left		3.24	
Krems-Hundssteig 2000-2002	HU-69/6	reindeer *(Rangifer tarandus)*	Femur	bone	left		3.21	
Krems-Hundssteig 2000-2002	HU-211/2	reindeer *(Rangifer tarandus)*	Calcaneus	bone	left		3.24	2
Krems-Hundssteig 2000-2002	HU-210/9	reindeer *(Rangifer tarandus)*	Astragalus	bone	left		3.24	
Krems-Hundssteig 2000-2002	HU-272/5	wolf *(Canis lupus)*	Metatarsus IV	bone	right		3.24	1
Krems-Hundssteig 2000-2002	HU-190/11	woolly mammoth *(Mammuthus primigenius)*	Astragalus	bone	right	subadult	3.24	
Krems-Hundssteig 2000-2002	HU-192/17	woolly mammoth *(Mammuthus primigenius)*	Astragalus	bone	right	subadult	3.24	
Krems-Hundssteig 2000-2002	HU-103/18	woolly mammoth *(Mammuthus primigenius)*	Astragalus	bone	right	subadult	3.24	
Krems-Hundssteig 2000-2002	HU-198/1	woolly mammoth *(Mammuthus primigenius)*	Astragalus	bone	right	subadult	3.24	5
Krems-Hundssteig 2000-2002	HU-184/27	woolly mammoth *(Mammuthus primigenius)*	Carpale 3	bone	right		3.24	
Krems-Hundssteig 2000-2002	HU-192/6	woolly mammoth *(Mammuthus primigenius)*	Phalanx	bone		infantile	3.24	

Krems-Hundssteig 2000-2002	HU-181/6	woolly mammoth *(Mammuthus primigenius)*	Capitatum	bone	left		3.24	
Krems-Hundssteig 2000-2002	HU-408/1	woolly rhinoceros *(Coelodonta antiquitatis)*		bone			3.23	2
Krems-Hundssteig 2000-2002	HU-348/9	woolly rhinoceros *(Coelodonta antiquitatis)*		bone			3.22	
Krems-Wachtberg 1930	KW-MK 923	hare *(Lepus* sp.*)*	Pelvis	bone				1
Krems-Wachtberg 1930	KW-MK 928	hare *(Lepus* sp.*)*	Metapodium	bone				
Krems-Wachtberg 1930	KW-MK 1070	horse *(Equus* sp.*)*	Long bones	bone				1
Krems-Wachtberg 1930	KW-MK 1105	ibex *(Capra ibex)*	Humerus	bone				1
Krems-Wachtberg 1930	KW-MK 917	muskox (*Ovibos moschatus)*	Phalanx 1, proximal	bone				1
Krems-Wachtberg 1930	KW-MK 931	arctic fox (*Vulpes lagopus)*	Ulna	bone	left			1
Krems-Wachtberg 1930	KW-MK 935	arctic fox (*Vulpes lagopus)*	Mandibula	bone	left			
Krems-Wachtberg 1930	KW-MK 936	arctic fox (*Vulpes lagopus)*	Humerus	bone	left			
Krems-Wachtberg 1930	KW-MK 932	red fox *(Vulpes vulpes)*	Mandibula	bone	right			3
Krems-Wachtberg 1930	KW-MK 933	red fox *(Vulpes vulpes)*	Mandibula	bone	right			
Krems-Wachtberg 1930	KW-MK 934	red fox *(Vulpes vulpes)*	Mandibula	bone	right			
Krems-Wachtberg 1930	KW-MK 938	red fox *(Vulpes vulpes)*	Radius	bone	right			
Krems-Wachtberg 1930	KW-MK 1008	reindeer (*Rangifer tarandus)*		bone				1
Krems-Wachtberg 1930	KW-MK 907	wolf (*Canis lupus)*	Manibula	bone	left	adult		5
Krems-Wachtberg 1930	KW-MK 908	wolf (*Canis lupus)*	Manibula	bone	left	adult		
Krems-Wachtberg 1930	KW-MK 909	wolf (*Canis lupus)*	Manibula	bone	left	adult		
Krems-Wachtberg 1930	KW-MK 910	wolf (*Canis lupus)*	Manibula	bone	left	adult		
Krems-Wachtberg 1930	KW-MK 911	wolf (*Canis lupus)*	Manibula	bone	left	adult		
Krems-Wachtberg 1930	KW-MK 976	wolverine (*Gulo gulo)*	Mandibula	bone	right	adult		3
Krems-Wachtberg 1930	KW-MK 974	wolverine (*Gulo gulo)*	Mandibula	bone	right	adult		
Krems-Wachtberg 1930	KW-MK 975	wolverine (*Gulo gulo)*	Mandibula	bone	right	adult		
Krems-Wachtberg 1930	KW-MK 1045	woolly mammoth (*Mammuthus primigenius)*	Long bones	bone				3
Krems-Wachtberg 1930	KW-MK 1034	woolly mammoth *(Mammuthus primigenius)*	Femur	bone	right			
Krems-Wachtberg 1930	KW-MK 1033	woolly mammoth (*Mammuthus primigenius)*	Femur	bone	left	juvenile		
Krems-Wachtberg 1930	KW-MK 1104	woolly mammoth (*Mammuthus primigenius)*	Femur	bone	right			
Krems-Wachtberg 1930	KW-MK 1107	woolly rhinoceros *(Coelodonta antiquitatis)*	Humerus	bone				1
Langenlois A	LK-F1/1076	hare *(Lepus* sp.*)*	Scapula	bone	left	adult		2

Langenlois A	LK-1209/DI	hare *(Lepus* sp.*)*	Pelvis	bone	left	juvenile		
Langenlois A	LK-B3/159	goose *(Anser* sp.*)*	Ulna, proximal	bone	right	adult		1
Langenlois A	LK-A5-B5/43	horse *(Equus* sp.*)*	Radius	bone	right	adult		2
Langenlois A	LK-1572	horse *(Equus* sp.*)*	Radius	bone	right			
Langenlois A	LK-D3/368	ibex *(Capra ibex)*	Metacarpus	bone	right	adult		5
Langenlois A	LK-E3/611	ibex *(Capra ibex)*	Metacarpus	bone	right	adult		
Langenlois A	LK-D1/1212	ibex *(Capra ibex)*	Metacarpus	bone	right	adult		
Langenlois A	LK-D3/369	ibex *(Capra ibex)*	Metacarpus	bone	right	adult		
Langenlois A	LK-G1/799	ibex *(Capra ibex)*	Radius, distial	bone	left	juvenile		
Langenlois A	LK-E3/625	red deer *(Cervus elaphus)*	Mandibula, I3	bone	right	adult		1
Langenlois A	LK-Rt-1	reindeer *(Rangifer tarandus)*	Os centroquartale	bone	left			2
Langenlois A	LK-Rt-2	reindeer *(Rangifer tarandus)*	Metatarsus, proximal	bone	left?			
Kammern-Grubgraben	KG 240	hare *(Lepus* sp.*)*	Mandibula	bone	right	adult	3	1
Kammern-Grubgraben	KG 627	hare *(Lepus* sp.*)*	Humerus	bone	right	adult	3	
Kammern-Grubgraben	KG 241	hare *(Lepus* sp.*)*	Metatarsus III	bone	right	adult	3	
Kammern-Grubgraben	KG 2542	hare *(Lepus* sp.*)*	Tibia, distal	bone	left	adult	3	
Kammern-Grubgraben	KG 2331	hare *(Lepus* sp.*)*	Calcaneus	bone	left	adult	3	
Kammern-Grubgraben	KG 1500	hare *(Lepus* sp.*)*	Tibia	bone		adult	3	
Kammern-Grubgraben	KG 76	hare *(Lepus* sp.*)*	Humerus	bone	left	adult	3	
Kammern-Grubgraben	KG 1024	hare *(Lepus* sp.*)*	Tibia	bone	right		3	
Kammern-Grubgraben	KG 1061	hare *(Lepus* sp.*)*	Calcaneus	bone	right	adult	3	
Kammern-Grubgraben	KG 872	hare *(Lepus* sp.*)*	Tibia	bone	left	adult	3	
Kammern-Grubgraben	KG 711	hare *(Lepus* sp.*)*	Mandibula	bone	left	adult	3	
Kammern-Grubgraben	KG 225	hare *(Lepus* sp.*)*	Radius	bone	left	adult	3	
Kammern-Grubgraben	KG 391	bison *(Bison* sp.*)*	Metatarsus III+IV	bone		adult	4	1
Kammern-Grubgraben	KG 1155	bison *(Bison* sp.*)*	I1	tooth	right	adult	3	
Kammern-Grubgraben	KG 2652	bison *(Bison* sp.*)*	Mandibula, Processus muscularis	bone	left	adult	3 or 4	

Kammern-Grubgraben	KG 2547	bison *(Bison* sp.*)*	Maxilla, Molar	tooth			2 or 3	
Kammern-Grubgraben	KG 754	brown bear *(Ursus arctos)*	I3	tooth	right	adult	3	1
Kammern-Grubgraben	KG 2672	goose *(Anser* sp.*)*	Ulna	bone		adult	3	1
Kammern-Grubgraben	KG 5	horse *(Equus* sp.*)*	Mandibulamolar	tooth		adult	3	
Kammern-Grubgraben	KG 10	horse *(Equus* sp.*)*	Metatarsus III	bone	right?	adult	1	
Kammern-Grubgraben	KG 44	horse *(Equus* sp.*)*	Os tarsi centrale	bone	left	adult	3	
Kammern-Grubgraben	KG 384	horse *(Equus* sp.*)*	Mandibula	bone	right	adult	2	
Kammern-Grubgraben	KG 14	horse *(Equus* sp.*)*	Maxilla	bone	right	adult	3	
Kammern-Grubgraben	KG 1282	horse *(Equus* sp.*)*	Phalanx 1 anterior or posterior	bone		adult	3	4
Kammern-Grubgraben	KG 1324	horse *(Equus* sp.*)*	Metatarsus III	bone		adult	3	
Kammern-Grubgraben	KG 1017	horse *(Equus* sp.*)*	Metacarpus III	bone		adult	2	
Kammern-Grubgraben	KG 1944	horse *(Equus* sp.*)*	Humerus	bone	right	infantile	3	
Kammern-Grubgraben	KG 955	horse *(Equus* sp.*)*	Maxilla	bone	right	adult	3	
Kammern-Grubgraben	KG 956	horse *(Equus* sp.*)*	Maxilla	bone	right	adult	3	
Kammern-Grubgraben	KG 912	horse *(Equus* sp.*)*	Maxilla	bone	right	adult	3	
Kammern-Grubgraben	KG 97	ibex *(Capra ibex)*	Phalanx 2 anterior o. posterior	bone		adult	4	
Kammern-Grubgraben	KG 214	ibex *(Capra ibex)*	Phalanx 2 anterior o. posterior	bone		adult	3	
Kammern-Grubgraben	KG 385	ibex *(Capra ibex)*	Tibia	bone	right	adult	3	
Kammern-Grubgraben	KG 1288	ibex *(Capra ibex)*	Phalanx 2, posterior	bone		adult	4	3
Kammern-Grubgraben	KG 149	ibex *(Capra ibex)*	Mandibula	bone	right	infantile	3	
Kammern-Grubgraben	KG 249	ibex *(Capra ibex)*	Mandibula	bone	right	adult	3	
Kammern-Grubgraben	KG 1286	ibex *(Capra ibex)*	Phalanx 2, posterior	bone		adult	3	
Kammern-Grubgraben	KG 1277	ibex *(Capra ibex)*	Phalanx 2, posterior	bone		adult	3	

Kammern-Grubgraben	KG 1613	ibex *(Capra ibex)*	Phalanx 2 anterior o. posterior	bone		infantile	1	
Kammern-Grubgraben	KG 454	ibex *(Capra ibex)*	Mandibula	bone	right	adult	3	
Kammern-Grubgraben	KG 1491	arctic fox *(Vulpes lagopus)*	Mandibula	bone	right	adult	3	2
Kammern-Grubgraben	KG 1485	arctic fox *(Vulpes lagopus)*	Mandibula	bone	left	adult	3	
Kammern-Grubgraben	KG 223	arctic fox *(Vulpes lagopus)*	Caninus	bone	left	adult	3	
Kammern-Grubgraben	KG 1488	arctic fox *(Vulpes lagopus)*	Cranium, M1 und M2	tooth	right	adult	3	
Kammern-Grubgraben	KG 2069	arctic fox *(Vulpes lagopus)*	Mandibula	bone	right	adult	3	
Kammern-Grubgraben	KG 804	red deer *(Cervus elaphus)*	Phalanx 2 anterior o. posterior	bone		adult	3	1
Kammern-Grubgraben	KG 826	red deer *(Cervus elaphus)*	Mandibula M2	tooth	left	adult	3	
Kammern-Grubgraben	KG 2606	red deer *(Cervus elaphus)*	Metatarsus, proximal	bone	left	adult	3	
Kammern-Grubgraben	KG 1949	red deer *(Cervus elaphus)*	Maxilla Caninus	tooth			3	
Kammern-Grubgraben	KG 239	red fox *(Vulpes vulpes)*	Maxilla	bone	left	adult	3	1
Kammern-Grubgraben	KG 1	reindeer *(Rangifer tarandus)*	Antlers	antlers		adult	3	8
Kammern-Grubgraben	KG 3	reindeer *(Rangifer tarandus)*	Humerus	bone	right	juvenile/ subadult	3	
Kammern-Grubgraben	KG 4	reindeer *(Rangifer tarandus)*	Antlers	antlers		adult	3	
Kammern-Grubgraben	KG 6	reindeer *(Rangifer tarandus)*	Mandibula	bone	right	adult	3	
Kammern-Grubgraben	KG 7	reindeer *(Rangifer tarandus)*	Mandibula	bone	left	adult	3	
Kammern-Grubgraben	KG 8	reindeer *(Rangifer tarandus)*	Metatarsus III+IV	bone	right	adult	3	
Kammern-Grubgraben	KG 165	reindeer *(Rangifer tarandus)*	Mandibula	bone	right	subadult	3	
Kammern-Grubgraben	KG 261	reindeer *(Rangifer tarandus)*	Mandibula	bone	left	subadult	3	
Kammern-Grubgraben	KG 319	reindeer *(Rangifer tarandus)*	Humerus	bone	right	adult	3	
Kammern-Grubgraben	KG 327	reindeer *(Rangifer tarandus)*	Mandibula	bone	right	adult	3	
Kammern-Grubgraben	KG 375	reindeer *(Rangifer tarandus)*	Talus/Astragalus	bone	left	adult	1	
Kammern-Grubgraben	KG 376	reindeer *(Rangifer tarandus)*	Metatarsus III+IV	bone		adult	4	

Kammern-Grubgraben	KG 377	reindeer *(Rangifer tarandus)*	Os centroquartale	bone	right	adult	1	
Kammern-Grubgraben	KG 378	reindeer *(Rangifer tarandus)*	Metatarsus III+IV	bone		adult	4	
Kammern-Grubgraben	KG 379	reindeer *(Rangifer tarandus)*	Radius	bone	left	adult	3	
Kammern-Grubgraben	KG 163	reindeer *(Rangifer tarandus)*	Mandibula	bone	left	infantile	4	
Kammern-Grubgraben	KG 173	reindeer *(Rangifer tarandus)*	Mandibula	bone	right	adult	3	
Kammern-Grubgraben	KG 172	reindeer *(Rangifer tarandus)*	Mandibula	bone	right	adult	3	
Kammern-Grubgraben	KG 1618	reindeer *(Rangifer tarandus)*	Mandibula	bone	right	adult	2	
Kammern-Grubgraben	KG 1612	reindeer *(Rangifer tarandus)*	Mandibula	bone	right	juvenile	4	
Kammern-Grubgraben	KG 394	reindeer *(Rangifer tarandus)* (m.)	Antlers	antlers		adult	3	
Kammern-Grubgraben	KG 174	reindeer *(Rangifer tarandus)* (m.)	Mandibula	bone	right	juvenile	4	
Kammern-Grubgraben	KG 1063	wolf *(Canis lupus)*	Maxilla	bone	left		3	
Kammern-Grubgraben	KG 646	wolf *(Canis lupus)*	Mandibula, P4	tooth	left	adult	4	1
Kammern-Grubgraben	KG 2622	wolf *(Canis lupus)*	Mandibula I3	bone	left	adult	3	
Kammern-Grubgraben	KG 361	wolf *(Canis lupus)*	Mandibula, I3	tooth	left		4	
Kammern-Grubgraben	KG 1590	wolverine *(Gulo gulo)* (m.)	Mandibula	bone	left	adult	3	1
Kammern-Grubgraben	KG 2113	woolly mammoth *(Mammuthus pimigenius)*	Long bones	bone			3	
Kammern-Grubgraben	KG 2	woolly mammoth *(Mammuthus pimigenius)*	Long bones	bone		adult	3	
Kammern-Grubgraben	KG 38	woolly mammoth *(Mammuthus pimigenius)*	Long bones	bone		adult	3	
Kammern-Grubgraben	KG 1109	woolly mammoth *(Mammuthus pimigenius)*	Tibia	bone		adult	3	1
Kammern-Grubgraben	KG 1110	woolly mammoth *(Mammuthus pimigenius)*	Long bones	bone		adult	3	
Kammern-Grubgraben	KG 1111	woolly mammoth *(Mammuthus pimigenius)*	Radius	bone	right	adult	3	
Kammern-Grubgraben	KG 1113	woolly mammoth *(Mammuthus pimigenius)*	Long bones	bone		adult	3	

Supplementary Table S1. Isotopic and chemical results of the analysed material. A single measurement was carried out for sample 'HU-348/9'. The abbreviation 'n.d.' means 'not determined'. The absolute difference (AD) between individual measured values of a single sample are given for samples measured in duplicates (n=2). Standard deviations (SD) are given for all other samples measured in triplicates (n=3). At the bottom of the table, samples are listed that were not used in the evaluation (teeth samples, samples from AH 1/AL 1, and outliers as defined in the text). For rows labelled with 'X', values are missing.

Figure 1. Location of the study sites in Lower Austria. The study sites are indicated by red dots. A digital elevation model (DEM) in 10x10m resolution (www.data.gv.at/katalog/dataset/land-noe-digitales-hohenmodel-10-m#resources) served as base map.

Figure 2. Published radiocarbon data from (a) Krems-Hundssteig (Neugebauer-Maresch and Stadler, 2008; Händel, 2017), (b) Krems-Wachtberg (Heinrich, 1973; Einwögerer, 2000; Händel, 2017), (c) Langenlois A (Einwögerer, 2019), and from archaeological horizon (AH) 2 (d) and AH 1 (e) of Kammern-Grubgraben (Gilot, 1997; Haesaerts, 1990; Haesaerts et al., 2016; Händel et al., 2021a). All radiocarbon dates were re-calibrated with IntCal20 (Reimer et al., 2020) using OxCal version 4.4 (Bronk Ramsey, 2009). For comparison, the pollen assemblages of Bergsee (Duprat-Oualid et al., 2017) (f) and the soil development in the loess record of Nussloch (g) (Moine et al., 2017) are given as in Stojakowits et al. (2021). Lower panels show calcium (Ca^{2+}) as a measure of dust accumulation in Greenland (h) (note the inverse and logarithmic scale) (Mayewski et al., 1997; Rasmussen et al., 2014), $\delta^{18}O$ values (i) (Rasmussen et al., 2014), and temperature derived from $\delta^{15}N$ of entrapped air (j) (Kindler et al., 2014), all from the NGRIP record (Andersen et al., 2004; Rasmussen et al., 2014), reported on the Greenland Ice Core Chronology (GICC05; Andersen et al., 2006). Blue numbers in Ca^{2+} record represent Greenland Interstadials (GIS).

Figure 3. FTIR spectra of (a) bone powder and (b) extracted bone collagen of the same samples HU, KW, LK, and KG, respectively. Note that y-axis is arbitrary.

Figure 4. $\delta^{13}C$ and $\delta^{15}N$ bone collagen values of (a) Early Gravettian/pre-LGM sites KW+HU (33-31k cal a BP), (b) Early Gravettian/pre-LGM site LK (31-29k cal a BP), and (c) Early Epigravettian/LGM site KG (24-20k cal a BP). Mean values are represented as big squares in (a) for KW+HU, as big stars in (b) for LK, and big circles in (c) for KG. Whiskers represent the respective standard deviations. Small symbols indicate values of the respective study site, with triangles=HU, diamonds=KW, stars=LK, and circles=KG.

Figure 5. Box plots of most common herbivore $\delta^{15}N$ (a) and $\delta^{13}C$ (b) values of KW+HU (dark grey) and LK (light grey) in comparison to KG (white). Only taxa with n>3 are shown. Boxes represent 25 and 75 percentiles, open squares means, horizontal lines medians, whiskers standard deviations and black diamonds outliers. Stars indicate probability values that the null hypothesis ("values in both time periods are indifferent") can be rejected (*** $p<0.001$, ** $0.001<p<0.01$, * $0.01<p<0.05$).

Figure 6. Standard ellipse areas (SEA) (solid lines) and convex hulls (dashed lines) of different herbivores from (a) Early Gravettian/pre-LGM food webs KW+HU and LK (ibex) (33-29k cal a BP) and (b) Epigravettian/LGM food web KG (24-20k cal a BP). Lower panels are density plots of SEA of (c) Early Gravettian/pre-LGM food webs KW+HU and LK (ibex), and (d) Epigravettian/LGM food web KG. Black circles are mode values of the SEAb values, i.e., standard ellipse area calculated using a Bayesian approach. Grey boxes represent 50, 75, and 95% credibility. Red crosses are SEAc values that are SEA values corrected for sample size. For the number of specimens see Figure 5.

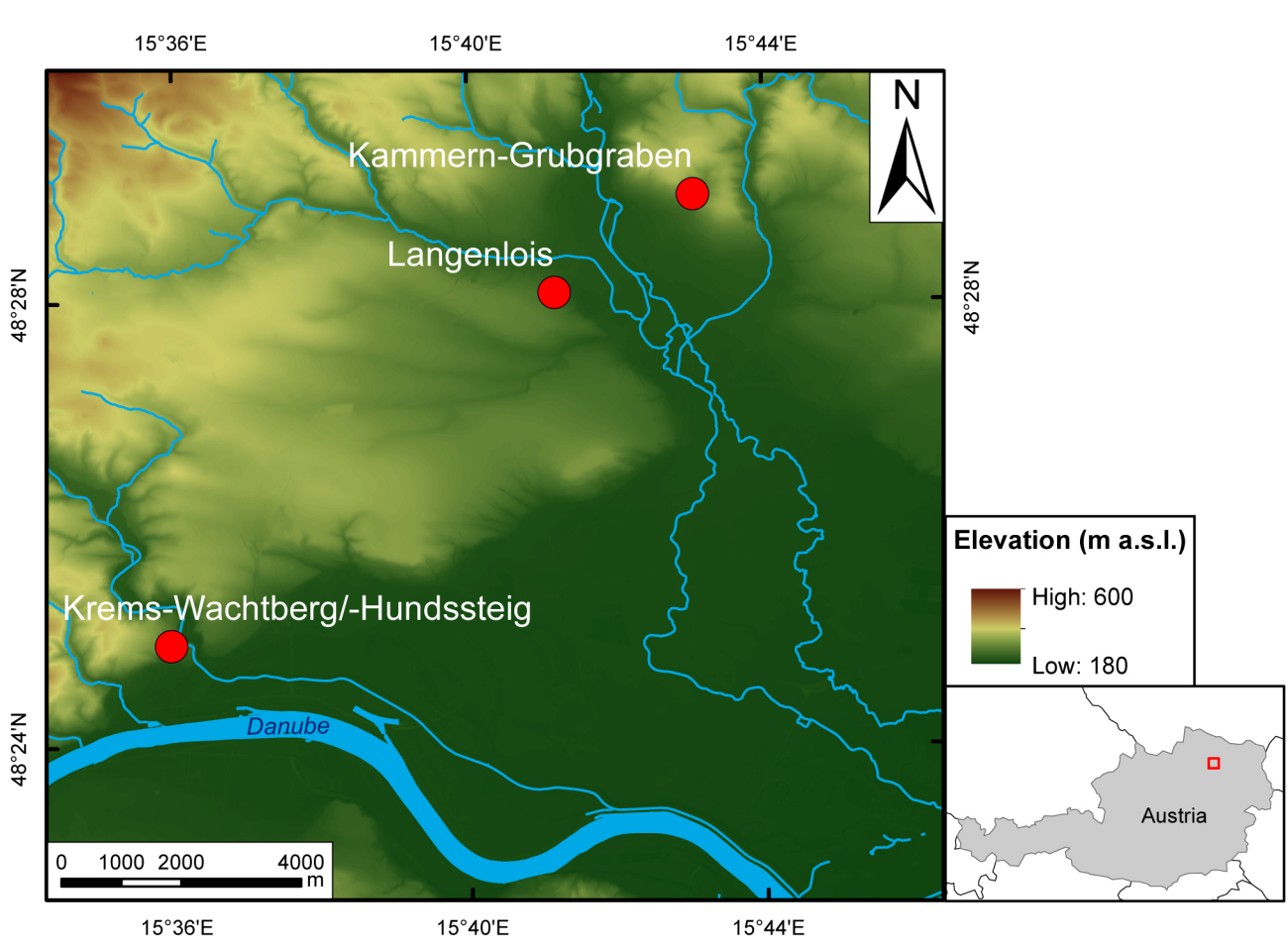
15°36'E
15°40'E
15°44'E
48°28'N
48°24'N
N
Kammern-Grubgraben
Langenlois
Krems-Wachtberg/-Hundssteig
Danube
0 1000 2000 4000
m
Elevation (m a.s.l.)
High: 600
Low: 180
Austria

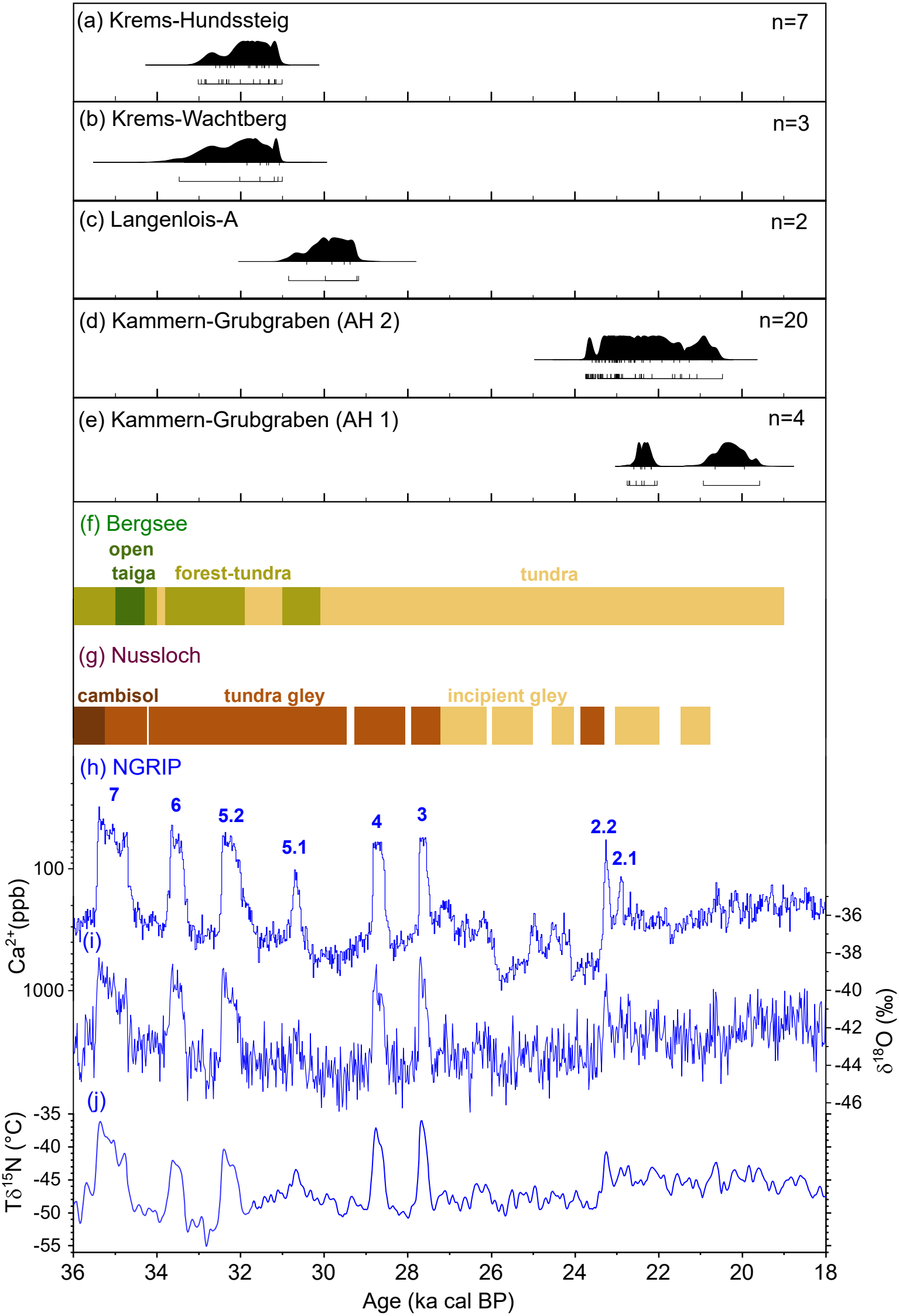
(a) Krems-Hundssteig
n=7
(b) Krems-Wachtberg
n=3
(c) Langenlois-A
n=2
(d) Kammern-Grubgraben (AH 2)
n=20
(e) Kammern-Grubgraben (AH 1)
n=4
(f) Bergsee
open
taiga
forest-tundra
tundra
(g) Nussloch
cambisol
tundra gley
incipient gley
(h) NGRIP
7
6
5.2
5.1
4
3
2.2
2.1
(i)
(j)
Ca2+(ppb)
100
1000
δ18O (‰)
-36
-38
-40
-42
-44
-46
TδN15 (°C)
-35
-40
-45
-50
-55
36
34
32
30
28
26
24
22
20
18
Age (ka cal BP)

(a)

reindeer
mammoth
horse
ibex
hare
musk ox
red deer
rhinoceros
goose
arctic fox
red fox
wolf
wolverine

δ^{15}N vs AIR

12
10
8
6
4
2
0

−22.0 −21.5 −21.0 −20.5 −20.0 −19.5 −19.0 −18.5 −18.0

δ^{13}C vs VPDB

(b)

reindeer
horse
ibex
hare
red deer
goose

δ^{15}N vs AIR

12
10
8
6
4
2
0

−22.0 −21.5 −21.0 −20.5 −20.0 −19.5 −19.0 −18.5 −18.0

δ^{13}C vs VPDB

(c)

reindeer
mammoth
horse
ibex
hare
bison
red deer
goose
arctic fox
red fox
wolf
wolverine

δ^{15}N vs AIR

12
10
8
6
4
2
0

−22.0 −21.5 −21.0 −20.5 −20.0 −19.5 −19.0 −18.5 −18.0

δ^{13}C vs VPDB

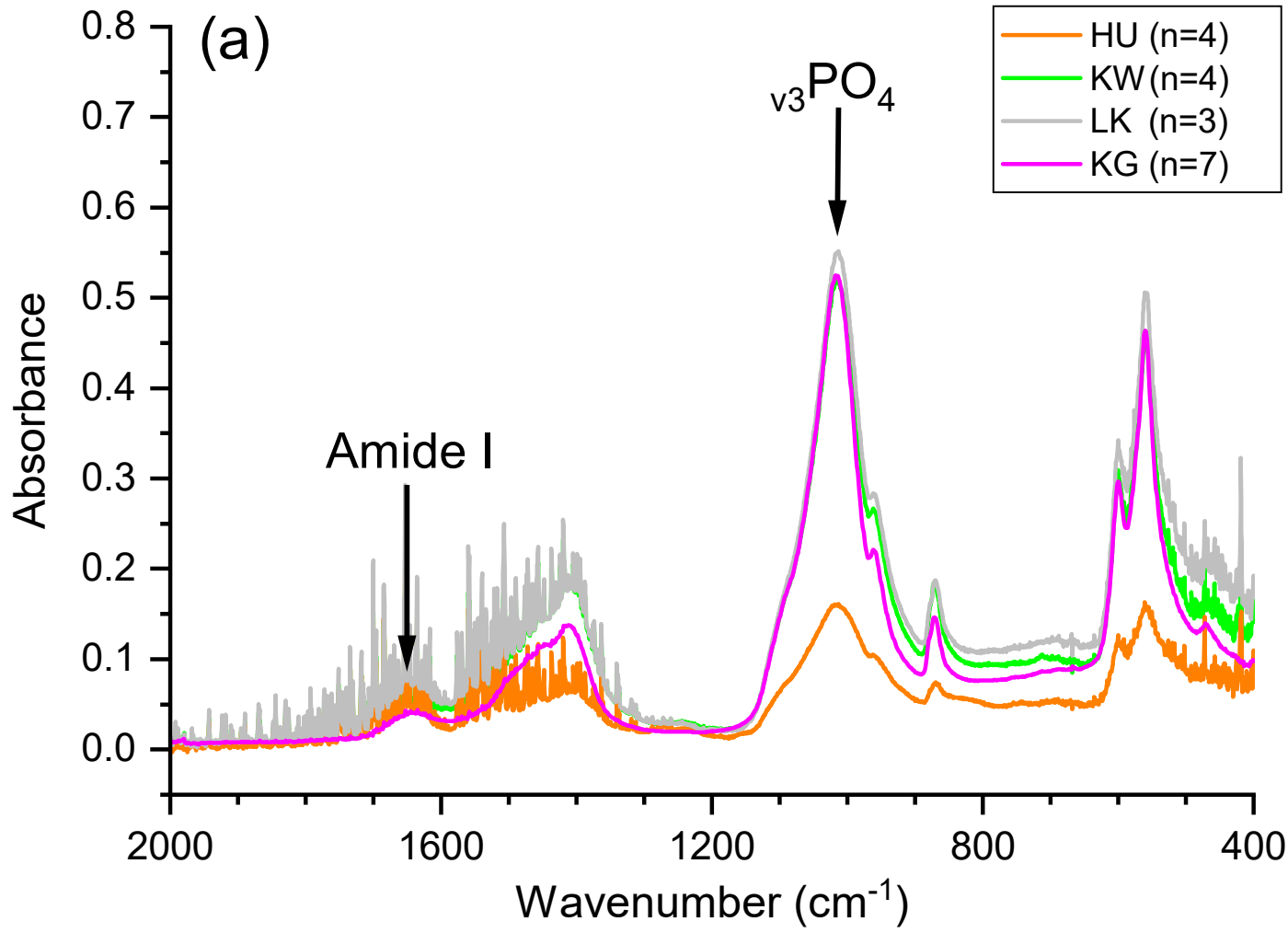
(a)
HU (n=4)
KW (n=4)
LK (n=3)
KG (n=7)
$_{v3}PO_4$
Amide I
Absorbance
Wavenumber (cm^{-1})
0.0
0.1
0.2
0.3
0.4
0.5
0.6
0.7
0.8
2000
1600
1200
800
400

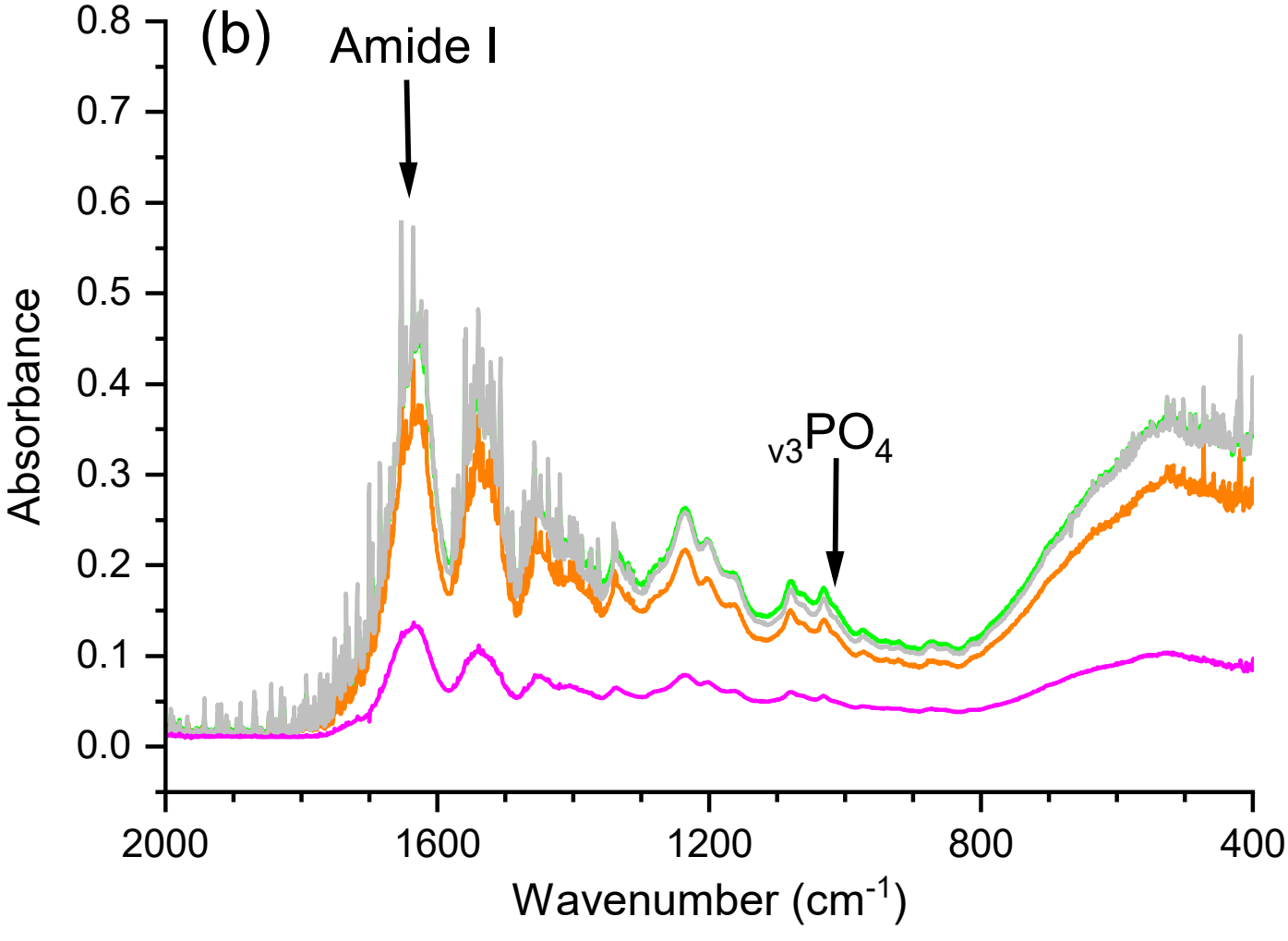
(b)
Amide I
$_{v3}PO_4$
Absorbance
Wavenumber (cm^{-1})
0.0
0.1
0.2
0.3
0.4
0.5
0.6
0.7
0.8
2000
1600
1200
800
400

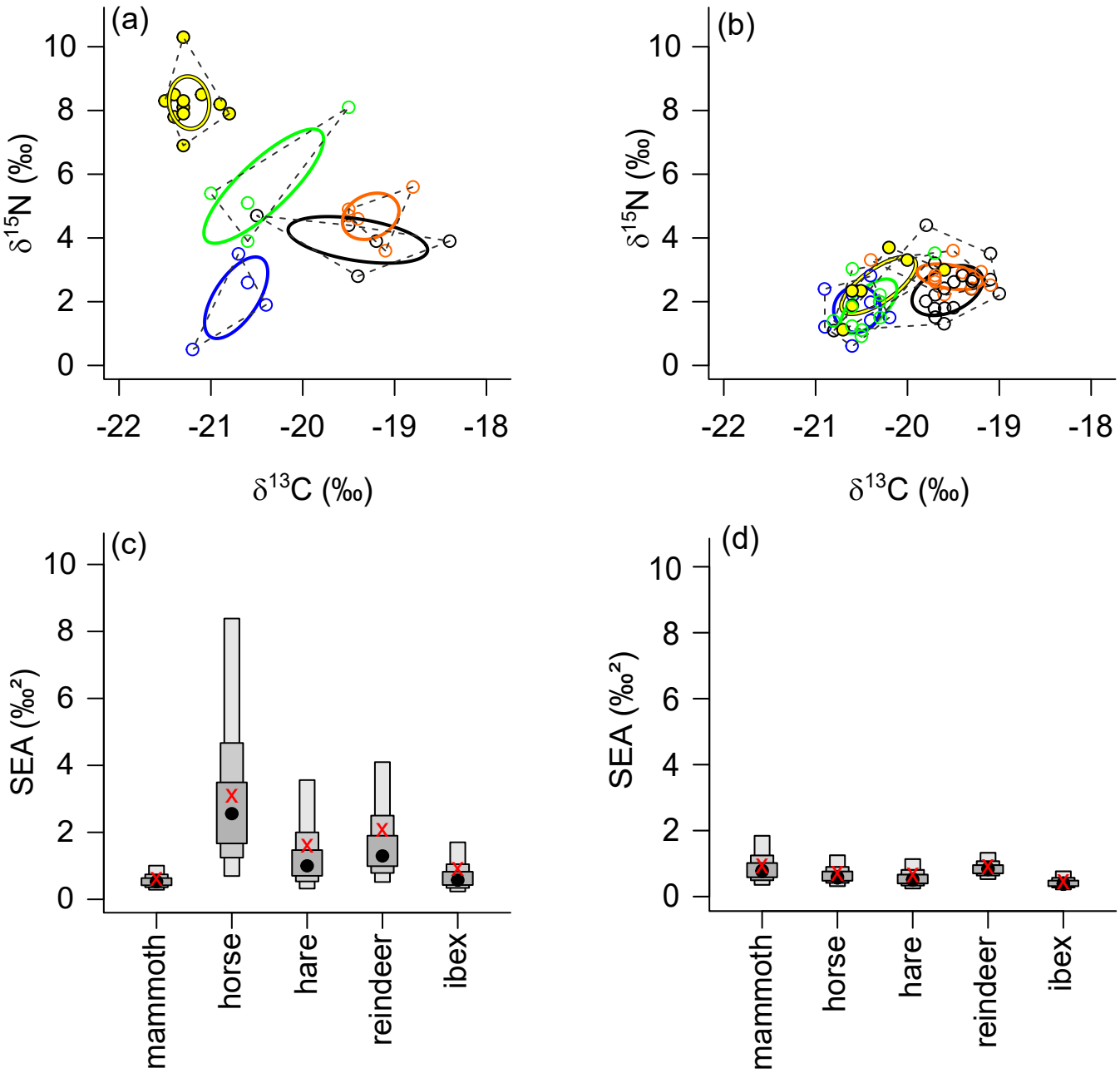
(a)
(b)
(c)
(d)
δ15N (‰)
δ13C (‰)
SEA (‰²)
-22
-21
-20
-19
-18
0
2
4
6
8
10
mammoth
horse
hare
reindeer
ibex

(a)

***

**

**

**

KW + HU
LK
KG

$\delta^{15}N$ (‰)

12
10
8
6
4
2
0

mammoth (n=11)
mammoth (n=7)
horse (n=4)
horse (n=10)
hare (n=4)
hare (n=8)
reindeer (n=5)
reindeer (n=20)
ibex (n=5)
ibex (n=9)

(b)

***

$\delta^{13}C$ (‰)

−18
−19
−20
−21
−22

mammoth (n=11)
mammoth (n=7)
horse (n=4)
horse (n=10)
hare (n=4)
hare (n=8)
reindeer (n=5)
reindeer (n=20)
ibex (n=5)
ibex (n=9)